AGU PUBLICATIONS

JGR

Journal of Geophysical Research: Oceans

RESEARCH ARTICLE

10.1002/2017JC012931

Key Points:
- Seasonal variations in POM $\delta^{13}C$ and $\delta^{15}N$ biogeochemistry were investigated
- Seasonal dynamics of POM are governed by climate variability and extreme events
- Effect of seasonal flooding on POM cycling is apparent at mid-salinities

Supporting Information:
- Supporting Information S1
- Table S1

Correspondence to:
F. Ye,
yefeng@gig.ac.cn

Citation:
Ye, F., W. Guo, Z. Shi, G. Jia, and G. Wei (2017), Seasonal dynamics of particulate organic matter and its response to flooding in the Pearl River Estuary, China, revealed by stable isotope ($\delta^{13}C$ and $\delta^{15}N$) analyses, *J. Geophys. Res. Oceans*, *122*, 6835–6856, doi:10.1002/2017JC012931.

Received 28 MAR 2017
Accepted 17 JUL 2017
Accepted article online 22 JUL 2017
Published online 29 AUG 2017

Seasonal dynamics of particulate organic matter and its response to flooding in the Pearl River Estuary, China, revealed by stable isotope ($\delta^{13}C$ and $\delta^{15}N$) analyses

Feng Ye[1,2], Wei Guo[2], Zhen Shi[3], Guodong Jia[4], and Gangjian Wei[1]

[1]State Key Laboratory of Isotope Geochemistry, Guangzhou Institute of Geochemistry, Chinese Academy of Sciences, Guangzhou, China, [2]Key Laboratory of Ocean and Marginal Sea Geology, Guangzhou Institute of Geochemistry, Chinese Academy of Sciences, Guangzhou, China, [3]State Key Laboratory of Tropical Oceanography, South China Sea Institute of Oceanology, Chinese Academy of Sciences, Guangzhou, China, [4]State Key Laboratory of Marine Geology, Tongji University, Shanghai, China

Abstract Nine cruises were conducted on a seasonal basis from 2013 to 2015 to investigate the spatial distribution and seasonal variability of $\delta^{13}C$ and $\delta^{15}N$ in particulate organic matter (POM), and its response to flooding in the Pearl River Estuary (PRE), south China. Our study reveals highly variable isotope ratios between seasons in this subtropical estuary, following seasonal climatic and hydrological cycles. Wet seasons had more isotopically depleted $\delta^{13}C$ values, indicating the dominance of terrestrial and freshwater algae POM, whereas the contribution from marine phytoplankton (16%–59%) was higher during the dry seasons. In contrast, $\delta^{15}N$ exhibited a sharp increase (up to 17.6‰) at low salinities (0–5) during high flow seasons. This was consistent with high NO_3^- concentrations, reflecting phytoplankton and bacteria assimilation of $\delta^{15}N$ enriched-NO_3^- as well as notable isotope fractionation during microbial mineralization. There was little annual variability in $\delta^{13}C$ over the 2 year period; however, particulate nitrogen (PN) exhibited lower concentrations but more enriched isotope values in 2015 than in 2014. This can be best explained by temperature-modulated biological processing of particulate organic nitrogen, partially due to different biogeochemical responses during normal (2014) and strong El Niño (2015) years. After flooding in June 2015, terrestrial organic matter and freshwater phytoplankton were the major components of POM within the estuary and shelf areas, whereas marine phytoplankton was the dominant component in the adjacent coastal waters with mid-salinities ($10 < S < 20$), as revealed by a phytoplankton bloom (>10 μg L^{-1}) and $\delta^{13}C$-enriched but $\delta^{15}N$-depleted POM.

1. Introduction

Estuaries are important zones for the production, transformation and removal of organic matter, both in dissolved and particulate form [e.g., *Hedges et al*., 1997; *Canuel and Hardison*, 2016]. Organic matter (OM) in estuaries is derived from autochthonous (in situ production) and allochthonous (e.g., terrestrial soils and urban sewage) sources. As compared to the dissolved organic matter (DOM), however, particulate organic matter (POM) is more bioavailable to organisms. Rivers export an estimated 0.14 Gt (10^{15} g) of particulate carbon and 0.02 Gt of particulate nitrogen (PN) to marine systems each year, of which 35% is in a labile form that is easily degraded by microbes [*Meybeck*, 1982; *Hedges et al*., 1997; *Seitzinger et al*., 2002]. Despite high OM loads, OM pools in the ocean have only minor terrestrial signatures based on measurements of carbon (C) isotopes and biomarkers (e.g., lignin phenols) [*Hedges et al*., 1997]. Therefore, it is essential to understand the origin, distribution and fate of POM that sustains the high levels of biological activity in estuaries, and which has important implications for regional and global carbon and nitrogen (N) cycles.

It is difficult to determine the origin of POM in estuaries because POM is supplied from multiple sources that change over time, including riverine inputs (e.g., terrestrial soils, C3 and C4 land plants) and in situ production by phytoplankton and bacteria as well as local sources from urban runoff and sewage effluent. Moreover, POM usually exhibits nonconservative behavior due to a number of mechanisms, including strong internal biogeochemical processes (e.g., phytoplankton production and bacterial respiration) and complex sedimentary dynamics during estuarine mixing. Thus, elucidating the sources and turnover of POM in estuaries is a challenging but necessary step toward effective estuarine management.

In aquatic systems, the C and N stable isotope ratios of POM (δ^{13}C and δ^{15}N) reflect the integrated influence of biogeochemical processes in the water column and sediments, including primary production, N transformation, and carbonate chemistry. Both sources (i.e., terrestrial soils, plankton of freshwater or marine origin) and internal cycling of POM can leave distinguishable signatures in the stable isotopic composition of POM, thus making δ^{13}C and δ^{15}N valuable tracers in tracking sources of POM and in understanding C and N cycling in aquatic systems [*Middelburg and Nieuwenhuize*, 1998; *Wu et al*., 2007; *Gao et al*., 2014]. However, in complex systems, such as river-dominated estuaries, overlapping stable isotopes and seasonal variability will hinder the characterization of POM sources to some extent. Despite these difficulties, it has been possible to infer major biogeochemical processes and sources of OM in estuaries using stable isotopes, particularly when these processes are tracked through an entire season or watershed.

The Pearl River, also known as the Zhujiang River, is the second largest river in China in terms of discharge volume. Over the past three decades, the lower reaches of the Pearl River have undergone rapid urbanization and extensive agricultural development, with heavy loads of anthropogenic waste being discharged into the river and estuarine system [*Zhang et al*., 1999; *Harrison et al*., 2008]. A number of studies have investigated the origin, abundance and bioavailability of dissolved nutrients and DOM in the Pearl River Estuary (PRE) [*Zhang et al*., 1999; *Callahan et al*., 2004; *Dai et al*., 2008a]. However, little is known regarding the dynamics, sources and cycling of POM in this complex estuarine system. For example, freshwater discharge and associated terrestrial loading was identified as the major source of POM by *Chen et al*. [1988, 1990], regardless of season. In contrast, *Yu et al*. [2010] noted distinct seasonal variation in particulate organic carbon (POC) sources, with in situ phytoplankton and terrestrial OM dominating in winter and summer respectively. Based on the combined analysis of carbon isotopes of POC and dissolved inorganic carbon (DIC), *Guo et al*. [2015] reported that POC was derived from highly degraded soils during the first phase of the wet season (i.e., spring), whereas it was relatively fresh and was of planktonic origin during the other seasons.

Overall, these studies are limited in the extent of their temporal monitoring (wet versus dry seasons) and no studies thus far have characterized the δ^{15}N, which could result in an incomplete understanding of how POM responds to seasonal and inter-annual perturbations. Moreover, several climate change impacts (e.g., increasing temperature and shifts in precipitation patterns) have ramifications for the mobilization, transport, processing, and deposition of OM in tropical and subtropical estuaries [*Liu et al*., 2007; *Chen and Jia*, 2009; *Maya et al*., 2011]. Among these impacts, flooding events, which are expected to be more frequent over the Pearl River Delta due to global warming [*Zhang et al*., 2012], have received particular attention. This is because most of the particulate and dissolved constituents that the river supplies to the sea are in response to episodic, high intensity events [e.g., *Sun et al*., 2007; *Tesi et al*., 2013]. Even though previous studies suggest that the export of material due to flooding has caused significant variations in the riverine environment (including water chemistry and particulate export) [e.g., *Sun et al*., 2007; *Zhang et al*., 2007], the investigations addressed the physical and biogeochemical responses to flood events are sparse in the PRE [*Dai et al*., 2008b; *Harrison et al*., 2008].

In this study, we conducted eight cruises between 2013 and 2015 to examine the temporal (mainly seasonal) variation in the chemical and isotopic composition of POM, and to identify the major mechanisms controlling this temporal variability. Furthermore, between May and June 2015, heavy precipitation over the Pearl River basin ($>$ 800 mm in Guangzhou, the highest on record since 1975) caused a large flood in the Pearl River system, with the maximum daily discharge (43,800 $m^3\ s^{-1}$) recorded on May 25 and a secondary maximum discharge (34,600 $m^3\ s^{-1}$) on June 17 (http://xxfb.hydroinfo.gov.cn). This provided a unique opportunity to investigate the short-lived impacts of flooding on POM dynamics and on the ecosystem of the PRE and adjacent coastal waters. Our hypothesis is that seasonally varying climate and hydrology likely alters the POM dynamics in this complex estuarine system, which is mainly regulated by rainfall, river discharge, and temperature-dependent biological processing.

2. Materials and Methods

2.1. Study Area

The PRE is a large subtropical estuarine system located midway along the northern coast of the South China Sea (SCS). The depth of the estuary varies mostly between 2 and 10 m (with an average of 4.8 m). The PRE receives riverine inputs from the Pearl River, which consists of three major tributaries (Xijiang, West River;

Beijiang, North River; Dongjiang, East River). Water discharge and suspended sediment load to the estuary is highly seasonal due to the warm and humid summer (southwest) monsoon and the cool and dry winter (northeast) monsoon, with about 80% of the water discharge and 95% of the sediment load being delivered during the wet season (April to September). The wet season can be further subdivided into the early flood period (April–June) and the late flood period (July–September), with the first being attributed to frontal precipitation, and the second being the result of tropical typhoons [*Luo et al*., 2008]. During the wet season, the interaction between high riverine discharge and seawaters from the SCS results in strong haloclinic stratification within the estuary, whereas in the dry season the water column is well-mixed due to the effect of reduced river discharge and strong northeasterly winds (wind speeds > 7 m s^{-1}). The PRE has three subestuaries (the Lingdingyang, Modaomen and Huangmaohai), among which the Lingdingyang is the largest, and it is traditionally known as the PRE. This study therefore focuses on the Lingdingyang and its upstream channels (the Huangpu Channel and Shiziyang channels), which receive about 50% of the Pearl River freshwater discharge. The residence time of the surface water in the estuary is less than 3 days during wet seasons and is extended to about 1–2 weeks during the dry seasons [*Yin et al*., 2000; *Sun et al*., 2014].

The drainage basin of the Pearl River covers an area of 453,700 km^2. The dominant activities in the upper drainage basin are forestry and agriculture, with the remainder being for urban use or barren [*Wei et al*., 2008; *Yu et al*., 2010]. The lower reaches (i.e., the Pearl River Delta) are dominated by agricultural land (~86%) and urban and industrial use [*Chen et al*., 2009]. The intensive use of reduced N fertilizers (i.e., urea and ammonium sulfate, 98% of the total fertilizer used) is widespread in the catchment around April. Moreover, the PRD is surrounded by a number of large metropolises like Guangzhou, Shenzhen, Hong Kong and Macau. The PRE, therefore, receives urban runoff, sewage inputs, and agricultural discharge from the surrounding areas. These high loads of organic matter and nutrients have a profound effect on the chemistry and biology of the system [*Harrison et al*., 2008 and references therein], which could in turn have strong influences on the sources and cycling of POM.

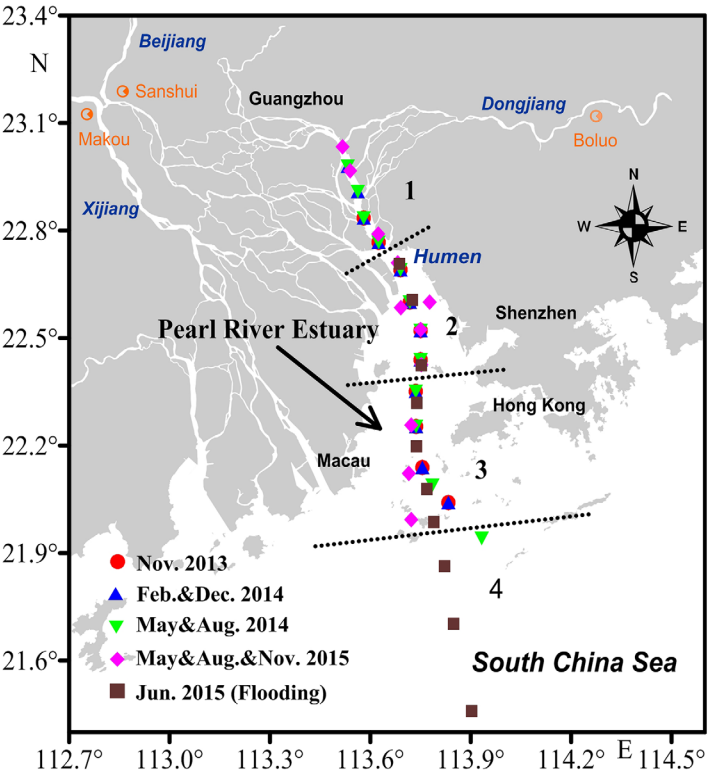

Figure 1. Map of the Pearl River Estuary and sampling sites for all cruises in 2013–2015. Orange circles denote the three main hydrological stations in the drainage basin. The estuary is divided into four zones: 1, upper reach; 2, upper estuary; 3, lower estuary; 4, shelf area.

2.2. Field Sampling

Seasonal observations (sampling twice for each season) were conducted between November 2013 and October 2015 along the estuary, from the river mouth to the coastal region near the Wanshan Islands (Figure 1 and Table 1). Each sampling transect comprised 10–16 stations ranging of depth 4–28 m. The site locations varied slightly among cruises, but we do not expect this variation to cause differences in chemical and biological processes among cruises. At each sampling site, surface water samples (0.5 m below the air water interface) were collected with a flow-through water-sampling bottle (5 L). Temperature and salinity data were recorded using a Valeport miniCTD (Valeport Ltd., Devon, UK) or SeaBird SBE 911 CTD meter (Sea-Bird Electronics, Inc. Bellevue, USA) that was calibrated before the cruise, with precisions of $\pm$ 0.01°C and $\pm$ 0.01 for temperature and

Table 1. Sampling Cruises for the Collection of Suspended Particulate Matter

Cruises	Date	Number of Samples	Other Supp. Parameters
GIG1	26–28 Nov 2013	10	Nutrient and stable isotopes
GIG2	23–26 Feb 2014	12	Nutrient and stable isotopes
GIG3	13–15 May 2014	12	Nutrient and stable isotopes
GIG4	3–5 Aug 2014	12	Nutrient and stable isotopes
GIG5	29–31 Dec 2014	12	Nutrient
SCSIO1	8–12 May 2015	11	Nutrient
PREPP	11–15 Jun 2015	10	Nutrient
SCSIO2	7–11 Aug 2015	11	Nutrient
SCSIO3	16–19 Nov 2015	11	Nutrient

salinity, respectively. Immediately after sampling, a known volume of water (range, 250–1500 mL) was filtered through precombusted (450°C, 4 h) and preweighed glass fiber filters (0.7 μm, Whatman GF/F). After filtration, the filters were rinsed with Milli-Q water to remove any salt, and then wrapped in aluminum foil and stored frozen at −20°C until further analysis.

The flood response sampling was conducted in the PRE and adjacent coastal waters (Figure 1) one week after the occurrence of the largest 2015 flood peak (floods of this magnitude have a return period of 5–20 years) over the Pearl River basin, which was recorded on the 25th to 27th of May in the lower reaches of the Pearl River, according to the local hydrological record. A total of 10 sampling stations were occupied over the study area, the locations of which are shown in Figure 1. It should be noted that the N–S transect along the PRE for this cruise is almost identical to the sampling stations for seasonal observations; therefore, it is possible to make a direct comparison of any biological and isotopic changes in estuarine waters induced by flooding. The suspended particulate matter (SPM) samples were collected and processed and other environmental parameters were measured in the same manner as those for the seasonal sampling (described above).

In addition to suspended particulate samples, surface sediment (0–5 cm) samples were collected using a Van Veen grab sampler in December 2014, and kept cold and in the dark prior to laboratory treatment.

2.3. Analyses

2.3.1. Environmental Parameters and Bulk Chemical Parameters

In the laboratory, the concentration of bulk SPM was estimated by the weight difference between the dried sample filters (oven dried at 50°C for 48 h) and their counterparts before filtration (25 or 47 mm Whatman GF/F filters). Nitrate (NO_3^-) and ammonium (NH_4^+) concentrations were analyzed on a Lachat QC8500 Flow Injection Autoanalyzer (Lachat Instruments, Loveland, USA) using standard colorimetric procedures [*Grasshoff et al*., 1999], with detection limits of 0.05 and 0.10 μmol L^{-1} for NO_3^- and NH_4^+ respectively [*Ye et al*., 2016]. *Chlorophyll (Chl a)* concentrations were determined spectrophotometrically according to *Lorenzen* [1967] after extraction into 90% acetone overnight.

POC and PN were determined by means of a CHNOS elemental analyzer (Elementar Vario) at the State Key Laboratory of Isotope Geochemistry, Guangzhou Institute of Geochemistry, Chinese Academy of Sciences, after de-carbonation of filters (25 mm diameter) with concentrated HCl in a vacuum-enclosed system. For surface sediments, aliquots of 1 M HCl were added to remove carbonate, and they were then freeze-dried and homogeneously crushed with a pestle and mortar before being analyzed for POC and PN. The precision for organic carbon and total nitrogen measurements was within 5%.

2.3.2. Isotope Analyses

For stable isotope analysis, the GF/F filters (47 mm diameter) containing particulate material were treated with concentrated HCl (36%) vapor in a desiccator to remove carbonates, and then oven dried at 50°C for 48 h after removing all traces of acid fumes in a clean laminar air flow. After de-carbonation, organic matter were scraped off the filters (or surface sediments), transferred into tin capsules, and analyzed using an elemental analysis isotope ratio mass spectrometer (EA-IRMS) (FlashEA1112 series elemental analyzer interfaced with a DELTA plus XL mass spectrometer). Isotopic ratios are reported in standard delta (δ) notation as permil (‰) relative to the Vienna PeeDee Belemnite standard (VPDB) for $^{13}C/^{12}C$, and atmospheric N_2 (air) for $^{15}N/^{14}N$. Standards were run every 6–10 samples, and precision for $\delta^{13}C$ and $\delta^{15}N$ measurement was ± 0.1‰ and ± 0.2‰, respectively.

2.4. Statistical Analyses

Pearson correlation analysis and a two-tailed significance test were performed using SPSS 16.0 to determine relationships between the measured parameters. Correlations were considered significant for $p < 0.05$. SPSS

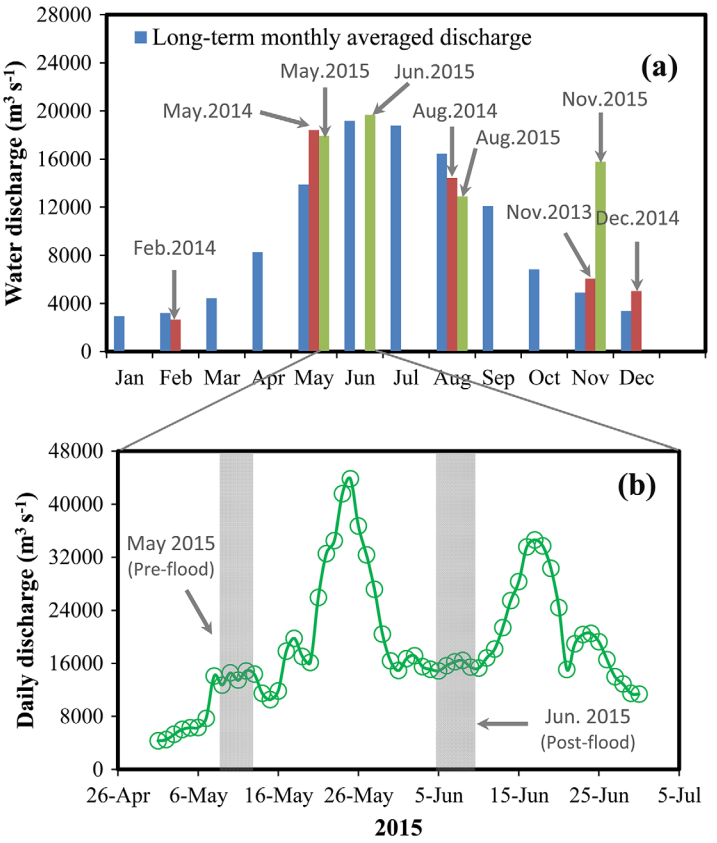

Figure 2. (a) Long-term monthly mean discharge for the Pearl River between 1959 and 2003 (blue bar) and discharge on observation months (red and green bars). (b) Daily discharge during the flood in May 2015. The average was calculated from discharge data measured at three main hydrological stations by the China Bureau of Hydrology via http://xxfb.hydroinfo.gov.cn.

was also used to run one-way analysis of variance to examine statistical differences in data between two or more groups.

3. Results

3.1. Hydro-Chemical Settings

The monthly averaged discharge of the Pearl River during our sampling months (seasonal observations) spanned a wide range, from 2664 to 19,669 $m^3\ s^{-1}$ (Figure 2a). In general, discharge during our observation periods had a similar seasonal pattern and magnitude to the long-term record (1959–2003), with higher flow rates from spring to summer, and lower flow rates from autumn to winter. November 2015 was an exception, with river discharge approximately 3 times (15,800 $m^3\ s^{-1}$) higher than that in the same period for normal discharge years (4900 $m^3\ s^{-1}$). This is likely a response to higher than average precipitation over the Pearl River watershed. Peak discharge over the 2 year period (2013–2015) is comparable at 18,418 and 17,923 $m^3\ s^{-1}$, and low discharge is slightly higher in December 2014 (5,020 $m^3\ s^{-1}$) than in the preceding winter (February 2014; 2664 $m^3\ s^{-1}$).

Concurrent with the Pearl River discharge, physical properties within the PRE also demonstrate a strong seasonal variability (Figure 3). Surface water temperatures were lowest (16–17°C) in winter and highest (29–31°C) in summer. In contrast, the median salinity in surface waters reached about 20.0 in winter, and dropped to less than 5.0 in late summer. It is surprising that salinity was slightly lower in autumn 2015 (average and standard deviation, 6.0 ± 8.3) compared with summer 2015 (6.5 ± 6.6), which is probably a result of the onset of high precipitation events across the watershed during this period (Figure 2). The averaged SPM concentrations ranged from 10 to 50 mg L^{-1}, with the highest concentrations associated with peaks in discharge but the lowest concentrations in winters.

Phytoplankton biomass, represented as *Chl a* concentrations, varied from 3.1 to 14.8 μg L^{-1}, with relatively high concentrations (> 5.0 μg L^{-1}) observed most frequently during warm seasons (spring/summer). The greatest *Chl a* concentrations were detected during summer 2014, when water temperatures were high. In spite of large seasonal differences, there are inter-annually consistent seasonal patterns for both NO_3^- and NH_4^+. NO_3^- concentrations were generally higher in wet seasons than in dry seasons, whereas NH_4^+ showed higher concentrations in winter than in other seasons. NO_3^- concentrations were significantly lower in 2013/2014 compared with 2014/2015, whereas NH_4^+ showed the opposite pattern, with higher values in 2013/2014 than in 2014/2015.

As compared with conditions before the flood (i.e., spring 2015, Figure 3), some physiochemical parameters (e.g., salinity and SPM concentrations) displayed no clear difference in the estuary during flooding. In the aftermath of the flood, however, nutrient (i.e., NO_3^- and NH_4^+) concentrations decreased to between half and

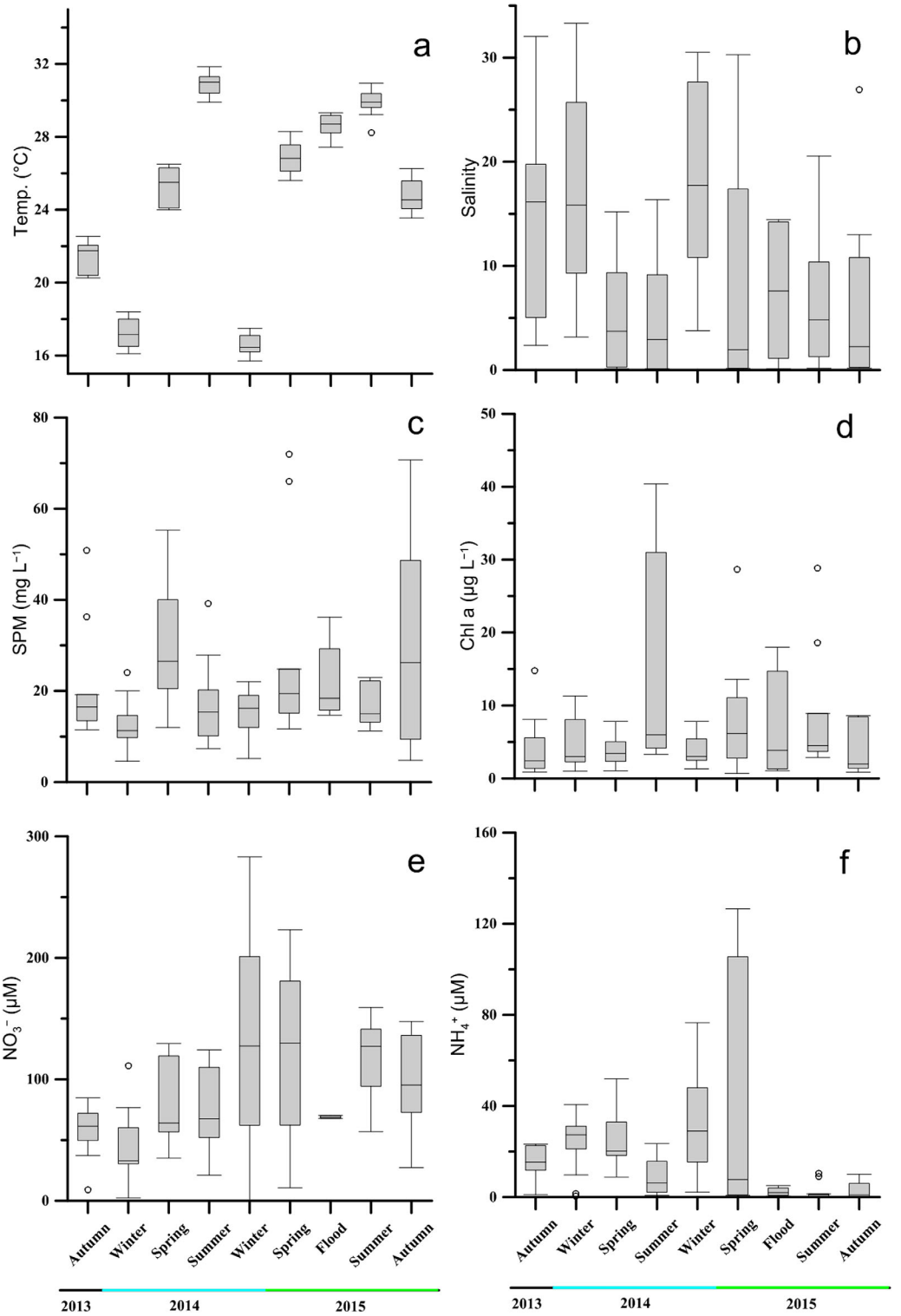

Figure 3. Variations in hydrographic parameters in surface water and bottom water samples from the PRE. Error bars represent standard deviations. For each box plot, the centerline represents the median, the box encompasses the 25th to 75th percentiles, and the bar denote the 5th and 95th percentiles; dots indicate the outliers.

one quarter of their preflood values and remained fairly constant. In contrast, we observed an apparent phytoplankton bloom in the lower estuary after the flooding, as illustrated by the significantly higher *Chl a* concentrations (up to 18.0 μg L^{-1} at a salinity of ~14.4).

3.2. Particulate Organic Carbon and Total Nitrogen

POC and PN in the PRE exhibited strong seasonal variability (Figure 4). The median POC concentrations varied by a factor of 3.1 (22.9–71.3 μM) in surface waters, whereas PN concentrations were more variable (varying by a factor of 5.3, 3.6–18.9 μM). In general, POC and PN concentrations were substantially higher during wet seasons than dry seasons. It should be noted that POC and PN concentrations in 2014 were considerably higher than those of 2015, with the exception of November 2015, which had higher concentrations than November 2014. When expressed as a percentage of SPM, we found that the median %POC and %PN during all nine cruises ranged from 3% to 7% and 0.4% to 2.2%, respectively, and they had similar seasonal patterns to the absolute concentrations. Percentages of organic carbon and total nitrogen in surface sediments of the PRE showed a similar pattern, and varied from 0.52% to 2.88% and from 0.07% to 0.23% respectively.

3.3. Isotopic Composition (δ^{13}C and δ^{15}N) of POM

The δ^{13}C and δ^{15}N of suspended particles in the PRE exhibited large seasonal variability, in particular for δ^{15}N (Figure 5). The δ^{13}C and δ^{15}N medians ranged from $-28.3‰$ to $-22.5‰$, and $3.0‰$ to $12.1‰$, respectively, with wet seasons being isotopically more depleted in δ^{13}C but enriched in δ^{15}N relative to dry seasons. These variations coincided consistently with seasonal changes in the distribution of *Chl a*, and in POC and PN concentrations (Figures 2 and 3). δ^{15}N in the surface water was $4.4‰$ heavier in spring 2015 than in

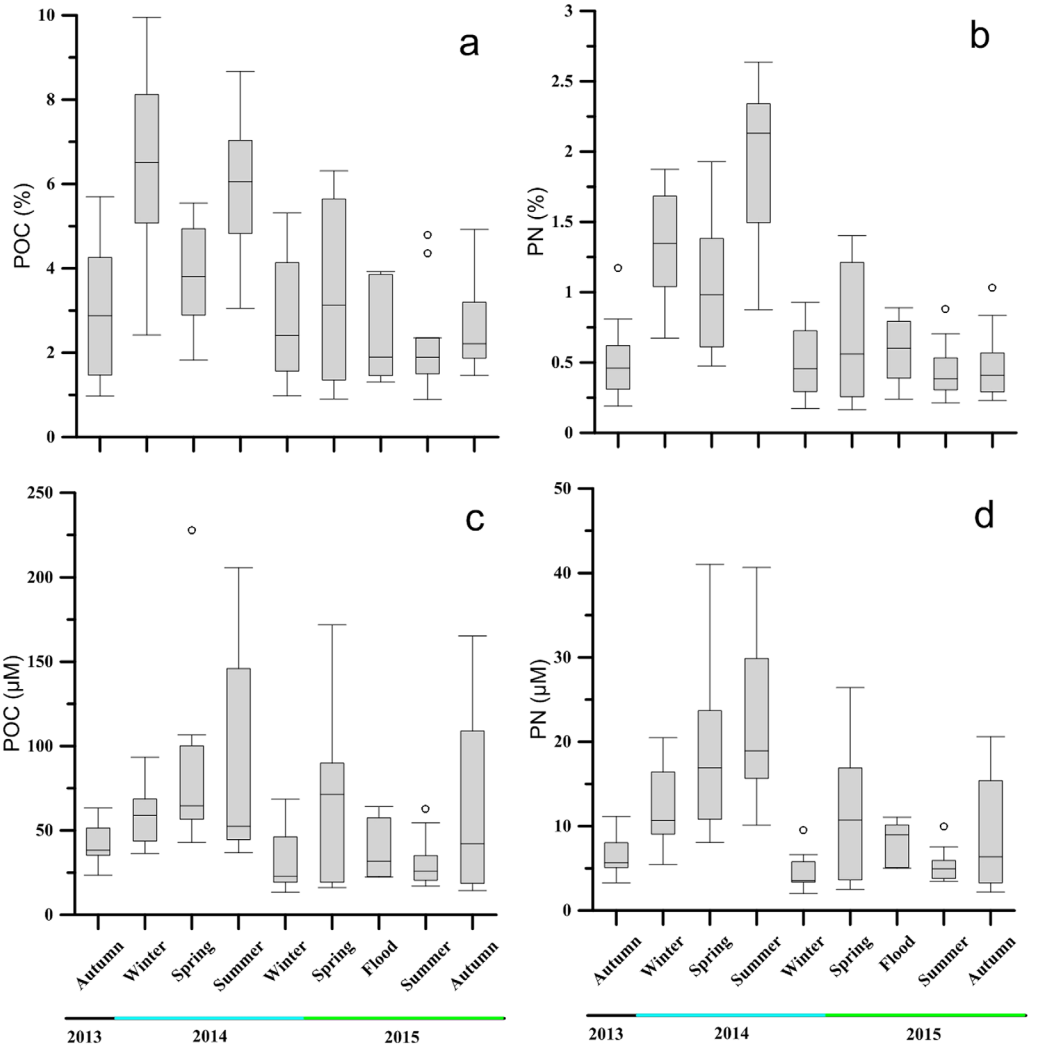

Figure 4. Seasonal variations in concentration and percentage of POC and PN in the PRE. For each box plot, the centerline represents the median, the box encompasses the 25th to 75th percentiles, and the bars denote the 5th and 95th percentiles; dots indicate the outliers.

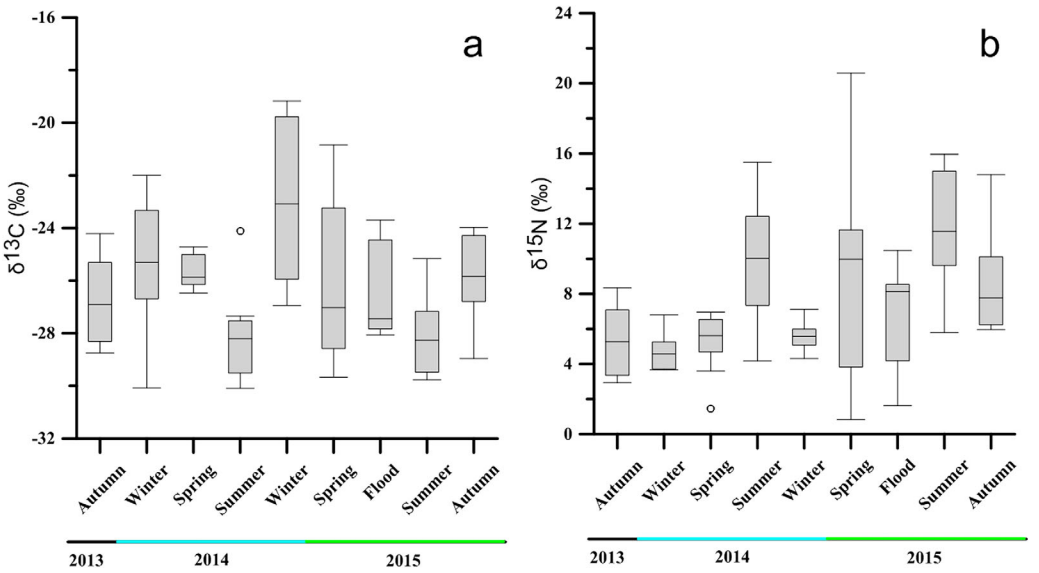

Figure 5. Seasonal variations of POM δ^{13}C and δ^{15}N in the PRE. For each box plot, the centerline represents the median, the box encompasses the 25th to 75th percentiles, and the bars denote the 5th and 95th percentiles; dots indicate the outliers.

spring 2014, whereas PN concentrations were more than 50% lower. However, there is no distinct difference in the seasonal pattern of δ^{13}C between 2014 and 2015. After the flood, the mean δ^{15}N of PN decreased by more than 3.0‰ relative to the value before the flood, whereas there was a less pronounced difference in the δ^{13}C of the particulate material. Overall, the δ^{15}N of POM is more variable than δ^{13}C in the samples studied, irrespective of the season.

Along the salinity gradient of the estuary, the δ^{13}C and δ^{15}N of POM in low-salinity waters varied substantially among seasons, with slightly heavier or more variable values commonly observed in periods of high river discharge (Figure 5). Further downstream (with increasing salinity) in each sampling transect, δ^{13}C of POM gradually increases from the upper estuary to the lower estuary. An exception here was the outmost stations in wintertime, which had even more depleted δ^{13}C values relative to the upstream stations. This is most likely linked to the existence of local δ^{13}C-depleted POM sources and/or biogeochemical processes (e.g., the sediment–water interaction and atmospheric deposition). There is no clear downstream trend in δ^{15}N for the entire system, although δ^{15}N shows a rapid increase in the early mixing stages (at salinities 0–5), where high phytoplankton biomass and bacterial abundance are often observed.

During the flood, the observed spatial distributions of δ^{13}C and δ^{15}N in the low salinity zone were consistent with those of the spring seasons and of November 2015, when another smaller flood occurred (Figures 6 and 7). Riverine POM in these periods was more enriched in δ^{13}C and δ^{15}N than in other seasons, suggesting that distinct sources of POM might exist [*Guo et al.*, 2015]. In contrast to the high δ^{15}N values (greater than 8‰) of POM throughout the estuary prior to the flood, δ^{15}N markedly decreased (from 8.3‰–10.5‰ to 1.6‰–4.2‰) at middle salinities, which coincided with heavier δ^{13}C values and significantly higher phytoplankton biomass after the flood. Thereafter, δ^{15}N increased rapidly to levels comparable with those in the low salinity zone, whereas δ^{13}C in the high salinity zone was highly variable and more negative than during other seasons.

The δ^{13}C of surface sediments ranged from −27.3‰ to −22.5‰, generally increasing from the upper reach to the lower estuary. In contrast, δ^{15}N remained fairly constant around 5.0‰ along the main axis of the estuary (Figure 6).

3.4. Statistical Analyses

In the present study, there are significant correlations between the seasonal isotopic composition (δ^{13}C and δ^{15}N) of POM and hydrographic (i.e., water temperature and salinity) and nutrient parameters (i.e., *Chl a*, NO_3^-, and NH_4^+), as shown in Table 2. In contrast, there are nonsignificant correlations between the isotopic

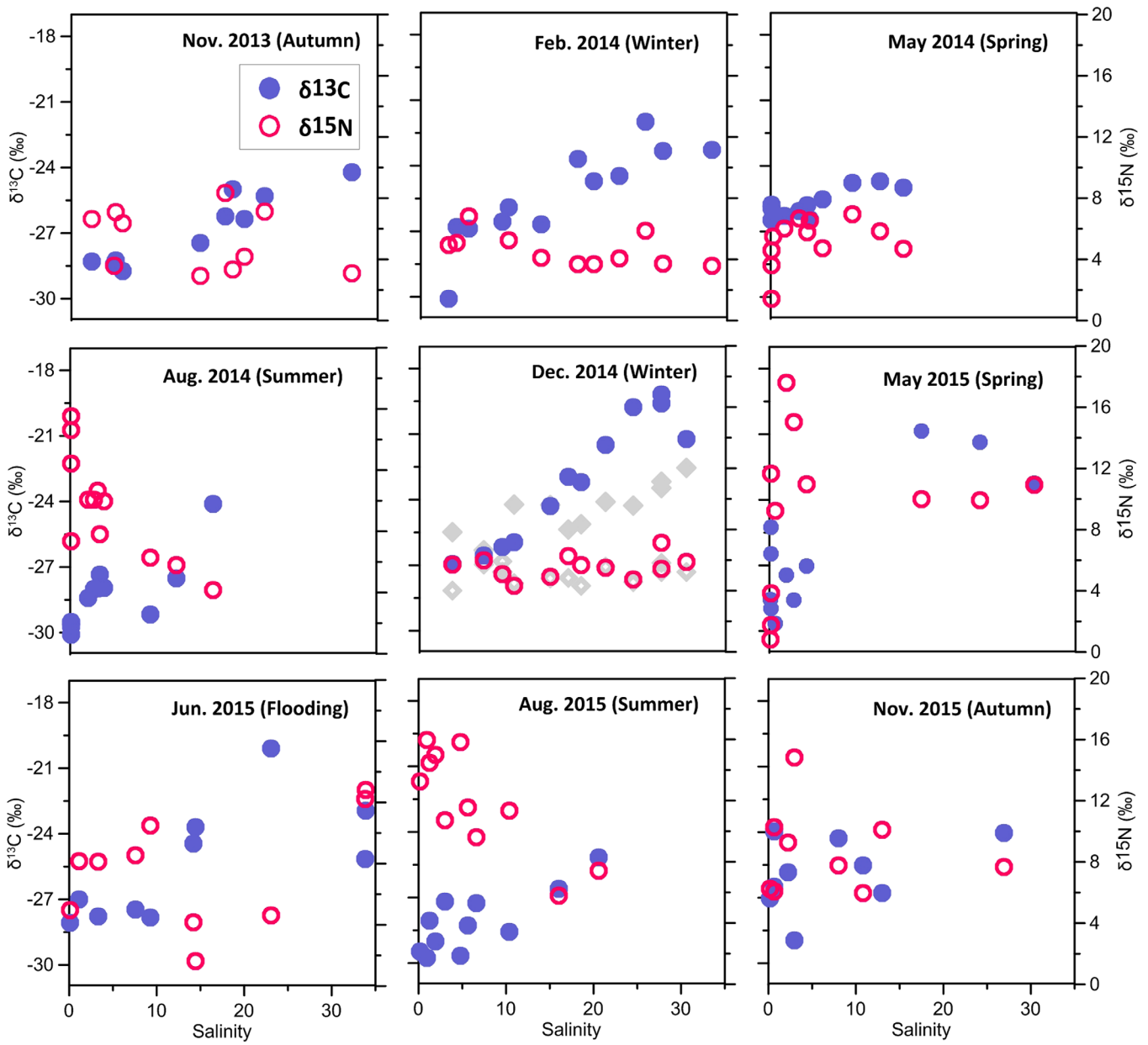

Figure 6. POM stable isotopes versus salinity in surface samples of the PRE for each cruise. The grey diamonds indicate δ^{13}C (filled) and δ^{15}N (open) values of surface sediments along the PRE sampled during December 2014.

composition of POM and its concentrations, water discharge, and SPM, which could be important controlling factors in the variability of the isotopic composition.

4. Discussion

4.1. Seasonal Variability in POM Sources

4.1.1. Seasonality of Riverine POM Sources

The PRE receives large quantities of terrestrial organic material from the Pearl River, which has highly variable environmental conditions (e.g., freshwater discharge and water temperature) that drive strong seasonality in riverine OM sources [*Callahan et al.*, 2004; *Chen et al.*, 2004; *He et al.*, 2010]. More than 90% of the annual suspended particulate load occurs during wet seasons (from April to September), mainly through

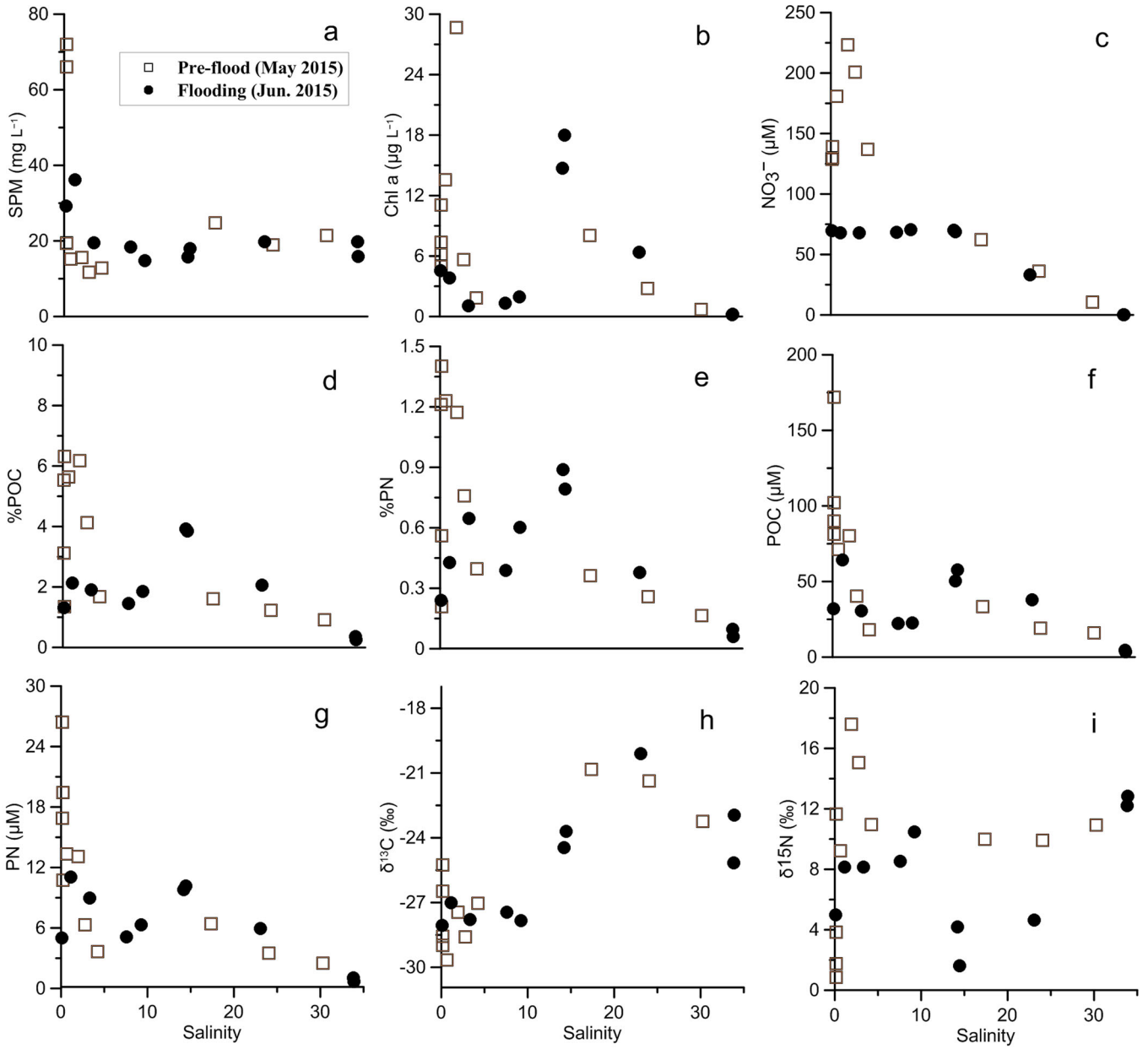

Figure 7. Hydrographic parameters, concentrations and isotopic compositions of POC and PN versus salinity both for pre- (open squares) and postflood (filled circles).

severe soil loss and erosion under intense rainfall, especially during periods of major flooding. Thus, SPM and POC carried by the river increases significantly during wet seasons (Figure 3).

It is of note that in this study, the freshwater samples ($S < 1.0$) for some of the seasons with high discharge rates ($>$ 15,000 $m^3\ s^{-1}$; spring and autumn) have more enriched POM $\delta^{13}C$ ($-29.7‰$ to $-24.0‰$) compared with samples collected during the late wet season ($-30.1‰$ to $-28.0‰$), whereas the opposite was observed for $\delta^{15}N$ (Figure 6). This difference is further evidenced by a significant correlation between POM $\delta^{13}C$ and SPM concentrations in all freshwater samples (Figure 8). There were also negative correlations between SPM concentrations and both %POC, and %PN for wet season samples. This is most likely related to the distinct OM sources and/or biogeochemical processes controlling POM cycling at different times during wet seasons. One possible explanation could be that there is more severe soil loss and erosion from surface environments during the early floods of wet seasons and/or under intense precipitation in the dry season (i.e., November 2015). As organic matter decomposition is limited during the dry season and litter

Table 2. Correlation Matrix (r) for the Seasonal Mean Particulate Organic Matter Concentrations and Isotopic Compositions, and Related Environmental Parameters During Different Cruises (n = 9) in Surface Waters of the Pearl River Estuary[a]

	Dis	T	S	SPM	*Chla*	NO_3^-	NH_4^+	POC	PN	$\delta^{13}C$	$\delta^{15}N$
Dis	1.00	0.80*	−0.88**	0.66	0.43	0.51	−0.70*	0.26	0.411	−0.51	0.56
T		1.00	−0.83**	0.23	0.63	0.56	−0.85**	0.09	0.42	−0.88**	0.83**
S			1.00	−0.57	−0.52	−0.64	0.74*	−0.39	−0.48	0.59	−0.72*
SPM				1.00	−0.23	0.24	−0.27	0.24	0.17	0.09	−0.03
Chla					1.00	0.47	−0.34	0.38	0.51	−0.56	0.72*
NO_3^-						1.00	−0.66	−0.01	−0.20	−0.43	0.81**
NH_4^+							1.00	0.12	−0.01	0.78*	−0.80**
POC								1.00	0.71*	−0.12	−0.07
PN									1.00	−0.33	0.09
$\delta^{13}C$										1.00	−0.72*
$\delta^{15}N$											1.00

*$p<0.05$; **$p<0.01$.

accumulates on surface soils, surface environments are characterized by enriched $\delta^{13}C$ (−28.3‰ to −21.7‰) [*Yu et al*., 2010] but depleted $\delta^{15}N$ (0.4‰ to 2.8‰) [*Fang et al*., 2011a], relative to other seasons. In addition, a significant elution of reduced N fertilizers that heavily applied around April due to high discharge could also play an important role in accounting for the low $\delta^{15}N$ values of river waters in spring seasons, because these fertilizers are characterized by ^{15}N-depleted values (−1.12 ± 1.44‰ for urea and −1.48 ± 1.38‰ for ammonium sulfate) in China [*Cao et al*., 1991]. Alternatively, summertime conditions of high terrestrial nutrient input and warm temperatures may promote enhanced freshwater phytoplankton growth relative to springtime [*Guo et al*., 2015]. POM produced by freshwater plankton is expected to have depleted-$\delta^{13}C$ (−28.4‰ to −32.6‰) but enriched $\delta^{15}N$ (> 6.7‰) compared with the corresponding soil-derived OM in the PRE [*Guo et al*., 2015; *Ye et al*., 2016]. These results are consistent with those in previous studies of other rivers/estuaries, such as the San Pedro River [*Brooks et al*., 2007] and the Mississippi River estuary [*Wang et al*., 2004].

Interestingly, we observed much higher concentrations of surface *Chl a* in freshwater during summer 2014 (30.1–40.4 μg L^{-1}) than summer 2015 (4.5–28.8 μg L^{-1}) (Figure 2). This difference is also shown by the much higher %POC and %PN (3.6%–8.7%) in summer 2014 as compared with the following year (0.9%–4.8%), likely indicating a greater contribution of freshwater algal-derived POM. However, both cruises observed similar $\delta^{13}C$ and $\delta^{15}N$ values, suggesting a significant contribution from the same source of POM

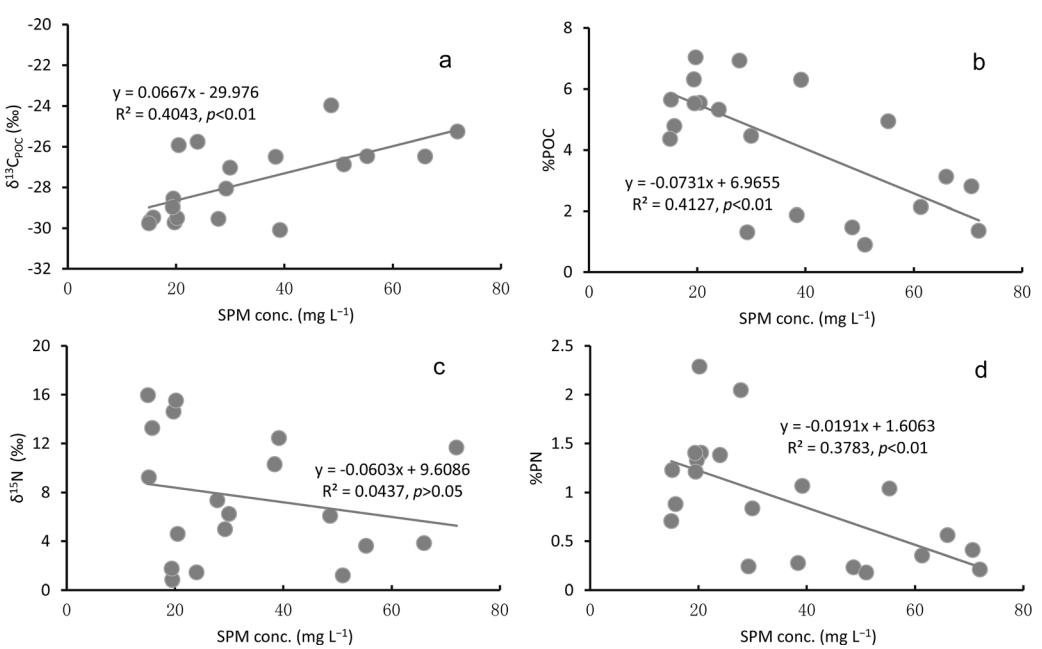

Figure 8. SPM concentrations versus %POC, %PN and their isotopic compositions for freshwater samples (S < 1.0) during wet seasons

in both years, probably from phytoplankton produced in situ. The accumulation of freshwater plankton has also been reported from other river/estuarine systems, for example, in the upper reaches of the Scheldt Estuary [*Kromkamp and Peene*, 1995]. Inter-annual climate variability could have caused the difference, which will be discussed below.

In the dry period, significant reductions in monsoonal precipitation and freshwater input reduced the flux of terrestrial organic material being washed into the PRE. This, combined with strong hydrodynamic conditions within the estuary that induced by seawater intrusion lead to much lower concentrations of SPM as well as POC and PN in dry seasons. In contrast, the in situ phytoplankton community has the potential to be more resilient to nutrient loading due to prolonged water residence times and increased light penetration, even at low temperatures [*Qiu et al*., 2010]. As a consequence, the POM carried by rivers is dominated by in situ phytoplankton (e.g., diatoms and green algae), as evidenced by the relatively more depleted δ^{13}C values (Figure 6) and low POC/*Chl a* ratios ($<$ 200) [*Guo et al*., 2015], which is a good indicator for the predominance of newly produced phytoplankton [*Cifuentes et al*., 1988]. November 2015 was an exception, when there was abnormally high precipitation and river discharge (Figure 2a), possibly related to the strong El Niño conditions in 2015, which reached peak intensity during November [*Zhai et al*., 2016]. For this time period, riverine POM was largely derived from the erosion of soil organic matter, as evidenced by the relatively enriched δ^{13}C values and high POC/*Chl a* ratios ($>$200).

4.1.2. POM Sources Within the Estuarine Region

The %POC and %PN decreased with increasing SPM concentrations, and significant relationships were seen between these parameters when pooling the whole data set. Specifically, most of the samples have higher %POC and %PN in SPM than the soils of the PRD (2.2% for POC and 0.2% for PN) [*Yu et al*., 2010], for low concentrations of SPM ($<$ 30 mg L^{-1}). This implies that rainfall-induced soil erosion from the catchment cannot alone account for the overall variability of POM within the estuary, and other OM sources and/or biogeochemical processes (e.g., in situ production of phytoplankton and resuspension of sediment) clearly contributed to the spatial and temporal changes in POM in the PRE. In contrast, when SPM concentrations exceeded 30 mg L^{-1} (mainly during flooding throughout the estuary), similar %POC and %PN measured for SPM and terrestrial soils indicates that the dominant source of POM during flooding seasons is from the flushing of soils in the drainage basin.

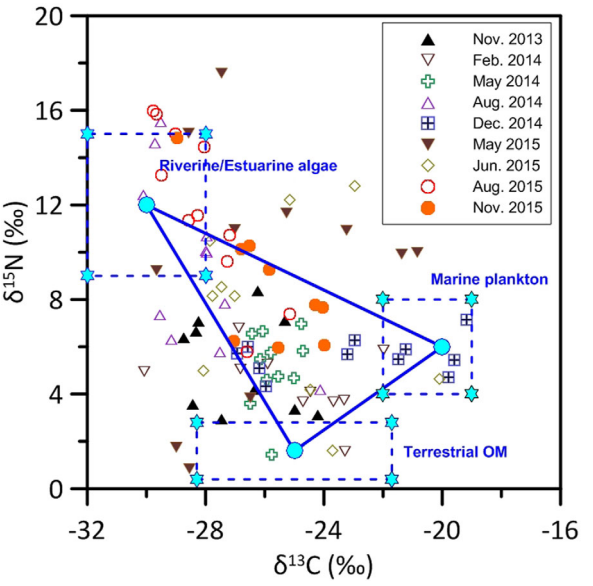

Figure 9. Mixing plots for POM δ^{13}C and δ^{15}N values from three potential sources for all samples in the PRE. Endmembers for POM sources (terrestrial OM, freshwater and marine phytoplankton) are indicated by solid cyan circles, where the dashed boxes represent the typical range of isotopic values for these POM sources.

Quantifying the relative contributions of organic matter from multiple sources is an important step toward our understanding of POM biogeochemistry in coastal marine environments. In this study, we identify that there are likely three major sources of OM, based on δ^{13}C and δ^{15}N (Figure 9), i.e., the terrestrial POM inputs, freshwater phytoplankton and marine sources, although other sources or processes might also be important. It is worth mentioning that POM derived from terrestrial soils and urban sewage sludge overlap in the δ^{13}C versus δ^{15}N plot, and therefore a comprehensive terrestrial end-member including soils and sewage sludge derived POM is assumed hereafter. Moreover, we note that δ^{15}N must be interpreted with caution as an organic tracer in the PRE, due to the kinetic isotope effects that occur during microbial mineralization and other related N biogeochemical processes [*Chen et al*., 2008; *Zhang et al*., 2014], which will be discussed in more detail in the next section. We calculate the relative

contribution of POM from these sources in each season using a three-endmember ($\delta^{13}C$) isotope mass-balance model (a similar two-endmember mixing model has been successfully applied to sedimentary OM identification in this area [*Hu et al*., 2006; *Yu et al*., 2010]).

$$\delta^{13}C_{obs} = \delta^{13}C_{terr} \times f_{terr} + \delta^{13}C_{fresh} \times f_{fresh} + \delta^{13}C_{mar} \times f_{mar} \quad (1)$$

$$f_{terr} + f_{fresh} + f_{mar} = 1 \quad (2)$$

where $\delta^{13}C_{obs}$ is the measured $\delta^{13}C$ value of a given sample; and $\delta^{13}C_{terr}$, $\delta^{13}C_{fresh}$ and $\delta^{13}C_{mar}$ are the carbon isotope ratios of terrestrial OM, freshwater algae, and marine OM, respectively. We used "Iso-Source" [*Phillips* and *Gregg*, 2001, 2003, 2005] to calculate the (ranges of) relative contributions of OM from terrestrial, fresh and marine phytoplankton sources to POM, although this does not provide a unique solution because there are three variables in two equations. In general, to graphically represent the data, the mean value of the range of contributions from each source was taken. We assumed $\delta^{13}C$ values of $-30.0 \pm 2.0‰$ and $-20.0 \pm 2.0‰$ for freshwater plankton and marine-derived POM, respectively, as suggested by previous studies [*Jia and Peng*, 2003; *Chen et al*., 2008; *Guo et al*., 2015]. A mean $\delta^{13}C$ value ($-25.0 \pm 3.3‰$) for different soils (-28.3–$21.7‰$) collected from the Pearl River drainage basin [*Yu et al*., 2010] and sewage sludge (-28.5–$21.0‰$) [*Maksymowska et al*., 2000; *Liu et al*., 2007] was taken as the terrestrial OM endmember.

Our results suggest that the POM within the PRE was sourced from terrestrial OM, freshwater algae and marine plankton derived from in situ biological production for all cruises. The most likely relative contributions from terrestrial inputs, newly produced freshwater, and marine plankton were found to be in the range of 18%–47%, 16%–73%, and 9%–52%, respectively (Figure 10). The greatest contribution from freshwater algae OM was recorded in summer (70%–73%) compared with other seasons (16%–52%). In contrast, the terrestrial contribution to the POM pool was significantly lower in summer (18%–20%) than in other seasons (32%–47%). The contribution of marine-derived OM decreased from 23%–52% in winter to 9%–10% in summer, showing the influence of marine plankton decreasing from dry seasons to wet seasons. The greater contribution of newly produced marine phytoplankton to the total POM pool in winter compared with other seasons most likely resulted from (1) a large decrease in terrestrial organic fluxes in winter, associated with a reduction in precipitation and soil erosion [*Yu et al*., 2010]; and (2) longer water residence times (~2 weeks) and increased light penetration due to low river discharge, which gives rise to marine phytoplankton production and accumulation within the estuary [*Rudek et al*., 1991; *Osburn et al*., 2012; *Dixon et al*., 2014]. It should be remembered that our estimate is a relative measure, and can reach high values even with a low overall mass of phytoplankton. In summary, elevated marine contributions occur during low discharge, whereas during high discharge, particularly at the onset of high precipitation, there are increased terrestrial and freshwater algal-derived POM inputs.

Spatially, the $\delta^{13}C$ values of POM in the PRE increased consistently from upstream ($-25.3‰$ to $-30.1‰$ at salinities < 1.0) to downstream in the estuary ($-19.2‰$ to $-23.3‰$ at salinities > 30.0) in all seasons, except for some samples collected from the outmost stations (Figure 6). This overall trend implies a decreasing terrestrial OM contribution to suspended POM, with an increasing contribution from marine POC seaward. However, for several seasons, there are still some anomalies in the overall distribution of $\delta^{13}C$ values versus salinity gradient. It is possible that the observed patterns are due to rapid changes in riverine and marine end-members [*Loder and Reichard*, 1981]. However, some of these discrepancies could indicate the active cycling of OM

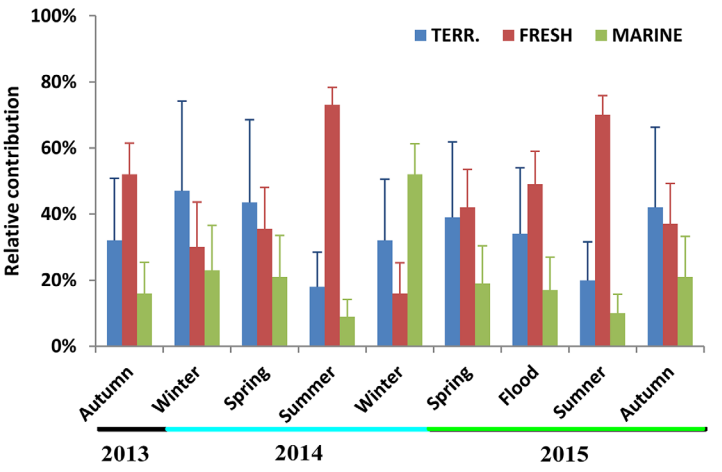

Figure 10. Seasonal mean of different sources contributing to estuarine POM (expressed as a percentage), estimated using a multiple source mixing model ("Iso-Source").

or external OM loading (e.g., sediment resuspension and atmospheric deposition). For example, during May 2015 and the subsequent flooding, POM had much more enriched $\delta^{13}C$ but depleted $\delta^{15}N$ at mid-salinities ($10 < S < 25$) relative to both upstream and downstream waters in waters. Even though both cruises could be strongly influenced by early floods, it is unlikely that rapid changes in concentration and isotope ratios of riverine POM could account for all of the observed patterns, as terrestrial inputs and freshwater algal-derived OM are characterized by more depleted $\delta^{13}C$, relative to marine inputs. Moreover, these anomalies coincided with abnormally high concentrations of *Chl a* (up to 18.0 $\mu g\ L^{-1}$) and elevated percentages of POC and PN, providing strong evidence for a greater contribution from marine OM. This could also explain the spatial distribution of $\delta^{13}C$ at the transition between the middle and high salinity zones during winter.

4.2. Factors Affecting POM Biogeochemical Processes and Seasonal Variations

4.2.1. Discharge as an Important Control on POM Isotopes

In this study, river discharge has a significant correlation with surface salinity and SPM for different seasons (Table 2), suggesting that discharge is the main factor controlling suspended sediment dynamics in the PRE. During periods of high discharge ($>$ 15,000 $m^3\ s^{-1}$), increased nutrient fluxes produce nutrient-rich conditions that are beneficial for algae growth and therefore result in higher phytoplankton production. However, the shorter residence time for water (several days) and higher turbidity due to high freshwater discharge could decrease reaction times and light availability for phytoplankton growth [*Yin et al*., 2000; *Harrison et al*., 2008]. The increase in suspended material is mostly derived from the erosion of terrigenous soils, which are characterized by very positive $\delta^{13}C$ but negative $\delta^{15}N$ values [*Wei et al*., 2008; *Yu et al*., 2010]. Hence, the fraction of OM derived from in situ algal biomass in brackish waters is expected to be low during wet seasons. This is also reflected by the slightly more enriched $\delta^{13}C_{POC}$ during early flooding than in other seasons (Figure 6).

Table 2 shows that the correlations between the isotope composition ($\delta^{13}C$ and $\delta^{15}N$) of POM and discharge (SPM) were low and not statistically significant ($p > 0.05$). This suggests that the link between discharge and POM dynamics is not straightforward, at least on a seasonal scale. Moreover, this could further indicate that other organic sources or biogeochemical processes, such as biological turnover and intense physical sediment–water interaction, play an important role in regulating the fate of POM in our study area.

4.2.2. Influence of Surface Water Temperature on POM Isotopic Signatures

The $\delta^{15}N$ of particulate material in estuaries, which is a complex pool of OM, is influenced by (1) POM sources, (2) the isotopic composition of the dissolved inorganic nitrogen (DIN) source, and (3) isotopic fractionation associated with N transformations. The $\delta^{15}N$ of POM was more complicated than the distribution of POM $\delta^{13}C$. The large variations in POM $\delta^{15}N$ along the salinity gradient cannot be due solely to the hydrodynamic mixing of multiple endmembers (Figure 9). During warm seasons (including the flooding events), POM had the most enriched $\delta^{15}N$ values (up to 17.6‰) in low-salinity waters (0–5, Figure 4), coinciding with the highest concentrations of NO_3^- and *Chl a*. Heavy $\delta^{15}N$ values (8.1‰–17.3‰) have also been reported for POM collected from other marine environments; e.g., the Tamar river estuary and the York River estuary [*Owens*, 1985; *McCallister et al*., 2004; *Hoffman and Bronk*, 2006].

There was a significant positive correlation between the relatively enriched POM $\delta^{15}N$ during warm seasons and NO_3^- concentrations, but a negative correlation between NH_4^+ concentrations (Table 2). Several processes can be invoked to explain the observed enrichment in $\delta^{15}N$, including (1) the influence of local urban runoff and sewage inputs (with enriched $\delta^{15}N$-DIN), and (2) OM from submarine groundwater (SGD) significantly affected by denitrification, and (3) phytoplankton (and bacterial) assimilation of $\delta^{15}N$-enriched DIN substrates and the subsequent microbial degradation. However, highly depleted $\delta^{15}N$ values (–1.1‰ to 3.3‰) have typically been reported for POM derived from local urban runoff and sewage effluents [*Sweeney et al*., 1980; *Thornton and McManus*, 1994; *Kendall et al*., 2001], although enriched POM $\delta^{15}N$ has also been observed. Moreover, precipitation and river runoff were generally high in wet seasons, which could dilute the contribution of domestic sewage inputs. We therefore expect that urban runoff/sewage inputs will not be the main driving force for isotopically enriched POM $\delta^{15}N$ in warm seasons.

SGD-derived N from the coastal area (i.e., the Pearl River Delta) could be a major source of isotopically enriched $\delta^{15}N$ for POM due to extensive denitrification occurring in groundwater. Previous research has shown that SGD can be an important potential contributor to total freshwater discharge, and the associated organic and nutrient inputs in the PRE [*Wang et al*., 2012; *Wang*, 2014]. Moreover, more isotopically enriched

δ^{15}N values of nitrate, the major constitute of DIN, were found in wet periods than dry periods (8.0‰–26.1‰ versus 6.9‰–19.8‰) as a result of the high denitrification rates in summer [*Zhao et al*., 2008]. However, the SGD-derived N can also be ruled out as the main cause of isotope enrichment, because groundwater should supply more DIN inputs during dry periods than wet periods ($0.34 \pm 0.29 \times 10^8$ versus $0.21 \pm 0.17 \times 10^8$ mol d^{-1}) [*Wang*, 2014].

Therefore, the isotopically heavy δ^{15}N of POM can be attributed to δ^{15}N-enriched DIN uptake by phytoplankton and bacteria, and associated microbial degradation. This hypothesis is supported by: (1) the elevated $\delta^{15}N_{PN}$ that coincides with the pronounced regional maximum in phytoplankton biomass (>10 μg L^{-1} *Chl a*) and SPM concentrations and (2) relatively high δ^{15}N values of NO_3^-, but relatively depleted dissolved organic nitrogen and NH_4^+ have been reported within the low salinity region of the PRE during wet seasons, mainly due to denitrification within the water column and/or throughout the watershed [*Chen et al*., 2009; *Ye et al*., 2016], and (3) high NO_3^- (> 100 μM) but low NH_4^+ concentrations (< 10 μM, data not shown) have been observed, which lead to the assumption that NO_3^- was the most important N substrate utilized by phytoplankton and bacteria in the upper estuary [*Li et al*., 2015; *Ye et al*., 2016]. The dominance of NO_3^- utilization has also been reported in the NO_3^--rich (up to 600 μM) Thames estuary by *Middelburg and Nieuwenhuize* [2000]. These data, therefore, indicate that the observed pattern was mainly due to the production of ^{15}N-enriched PN from an enriched NO_3^- pool and its subsequent remineralization.

In contrast, the δ^{15}N of POM is relatively depleted and fairly constant (around 6‰) along the salinity gradient in low discharge seasons than high discharge seasons. There are two reasons might be responsible for the observed distribution. (1) POM is transported with relatively little biological processing (e.g., assimilation and microbial degradation) due to the low temperatures during these times, and there are limited N isotope effects that occurs during POM transportation. (2) In the low discharge seasons, an increase in the relative contribution of sewage sludge load (with depleted δ^{15}N, < 2‰) [*Maksymowska et al*., 2000; *Liu et al*., 2007 and references therein; *Wu et al*., 2007] to the SPM pools relative to other sources would be expected, which could mask the δ^{15}N enrichments due to the assimilation of δ^{15}N-enriched DIN by freshwater phytoplankton.

In general, water temperature has a significant effect on pCO_2, the isotopic fractionation between HCO_3^- and CO_2 (aq), and phytoplankton growth rate. These three factors could result in the apparent positive correlation between $\delta^{13}C_{POC}$ and water temperature [e.g., *Rau et al*., 1991; *Lara et al*., 2010]. However, it was surprising that a significant anti-correlation ($r = -0.88$, $p < 0.01$) was observed between the average $\delta^{13}C_{POC}$ and water temperature in the PRE (Table 2). This is likely to be related to the negative correlation between water temperature and salinity (Table 2), and implies that the direct effect of temperature on $\delta^{13}C_{POC}$ is relatively minor compared with the influence of $\delta^{13}C_{DIC}$ in this region, which shows a strong correlation to salinity. This is consistent with the results reported for the hypertrophic Sumida River Estuary and Tokyo Bay [*Sato et al*., 2006].

On a seasonal scale, there was a positive correlation between the seasonal mean $\delta^{15}N_{PN}$ and water temperature (Table 2). Moreover, stepwise multiple linear regressions identified temperature as the single most important predictor of $\delta^{15}N_{PN}$. These results suggest that temperature has a profound effect on the temporal variations of $\delta^{15}N_{PN}$ in the PRE, mainly due to its effect on biologically mediated processes. It is known that $\delta^{15}N_{PN}$ of autochthonous POM is determined by the δ^{15}N values of available N substrates, isotopic fractionation during N assimilation, and the fractional utilization of N substrates [e.g., *Sigman et al*., 1999; *Sato et al*., 2006]. Hence, there are at least two possible explanations for the isotopically heavier PN that is observed at temperature increased: (1) biological assimilation of increasingly enriched δ^{15}N of N substrates (e.g., NH_4^+ and NO_3^-) at elevated temperatures and (2) rising temperatures affecting various N processes (e.g., assimilation and remineralization) and associated N isotope fractionations that take place within the water column or over the watershed, and are ultimately transported into the estuary.

Ammonium and NO_3^-, which are expected to be the major contributors to biological N demand, are the major components of the dissolved N pool in the PRE. NH_4^+ assimilation by phytoplankton was similar in magnitude to NO_3^- uptake, based on uptake incubation experiments [*Cai et al*., 2002; *Liu et al*., 2007]. Both N sources, therefore, should be taken into further consideration. Despite some difference in retention times of POM and nutrients exists, because the growth rates of a natural phytoplankton community may reach 2.4 d^{-1} in the regional subtropical waters like the PRE [*Yin et al*., 2000], water residence time of 1–2 days are

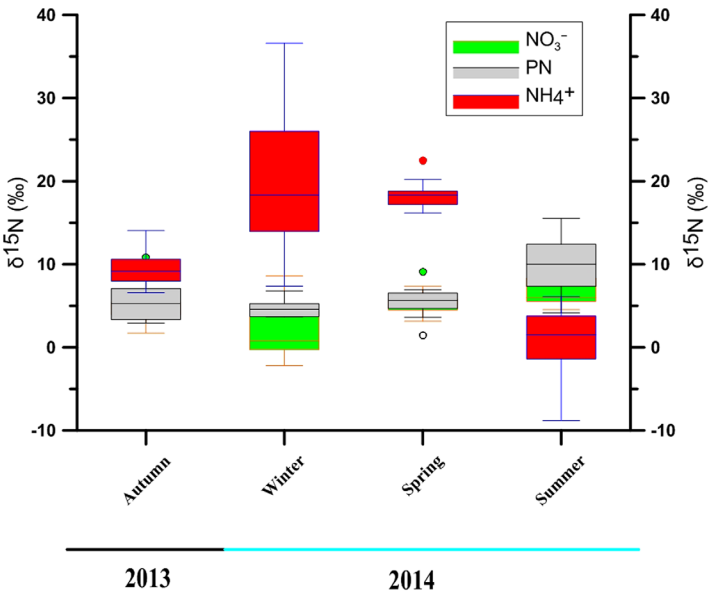

Figure 11. Comparison of seasonal variations in $\delta^{15}N$ values of NO_3^-, NH_4^+ and PN from autumn 2013 to summer 2014, including NO_3^- and NH_4^+ isotope data from *Ye et al.* [2016].

long enough to reach balance growth. Thus, we suggested that different forms of N and their isotopic values are important factors in controlling POM dynamics in the PRE.

Fortunately, simultaneous analysis of NH_4^+ and NO_3^- isotope values for the first four seasons [*Ye et al.*, 2016] allows us to better determine what role DIN assimilation played in the observed data. Marked decreases in $\delta^{15}N_{NH4}$ from winter to summer were (Table 2), indicating that seasonal viability of $\delta^{15}N_{NH4}$ did not exert a major influence within the estuary. This contradicts observations from the Delaware estuary and inner Tokyo Bay, in which the dependence of $\delta^{15}N_{PN}$ on water temperature has been ascribed to the potential seasonal differences in $\delta^{15}N_{NH4}$ values, despite these data not being available [*Cifuentes et al.*, 1988; *Sato et al.*, 2006]. Even when the significant N isotope fractionation that occurs during NH_4^+ assimilation (estimated using the empirical equation from *Liu et al.* [2013]; i.e., concentration-dependent N isotope fractionation during assimilation) is accounted for, a decrease in $\delta^{15}N$ of autochthonous POM would be expected if NH_4^+ were assumed to be the only N source, which again argues against $\delta^{15}N_{NH4}$ having a dominant role in POM $\delta^{15}N$ (Figure 11).

We note that $\delta^{15}N_{PN}$ had a positive correlation with NO_3^- concentrations and the $NO_3^-/(NO_3^- + NH_4^+)$ ratio, primarily due to the impact of active NO_3^- assimilation in the upper estuary, as mentioned above. In contrast to NH_4^+, the enrichment of $\delta^{15}N_{NO3}$, from a mean of 1.9‰ (n = 12) in winter to a mean of 6.7‰ (n = 12) in summer, has been detected in the estuarine waters of the PRE, and appears to be consistent with the seasonal pattern of $\delta^{15}N_{PN}$ (Figure 11). Nitrogen isotope fractionation during NO_3^- assimilation by marine diatoms is reported to be relatively uniform and independent of other environmental conditions under phosphorous (P) limitation [*Karsh*, 2014]. Phosphorus limitation is expected in the studied region, where P is considered a limiting nutrient [*Harrison et al.*, 2008]. A relatively constant ε_{NO3} value (–4.7‰ and −5.1‰ in summer and winter, respectively) provides strong supporting evidence for this hypothesis [*Ye et al.*, 2016]. Taking into account the N isotope effect during NO_3^- assimilation, a similar increasing trend with increasing temperature should also be expected. Collectively, NO_3^- assimilation could lead to a general increase in $\delta^{15}N_{PN}$ with increasing temperatures in seasonally variable estuary, while NH_4^+ uptake has the opposite effect, which, when combined, could result in relatively stable or decreasing $\delta^{15}N_{PN}$. Even though our calculation is only a rough estimate, we can conclude that the observed pattern between $\delta^{15}N_{PN}$ and temperature is not mainly due to planktonic assimilation of DIN substrates and associated N isotope fractionation.

An alternative mechanism for the temperature dependence of $\delta^{15}N_{PN}$ could be via the temperature-mediated microbial degradation of OM. Respiration rates are known to increase with increasing temperature (greater than the rate of increase of primary production), which could cause an increased supply of OM to bacteria, and ultimately lead to microbial degradation of OM [*Brown et al.*, 2004]. In detail, higher temperatures stimulate the growth of bacteria, bacterial biomass production and the activities of some sugar- and protein-degrading enzymes [*Pomeroy and Wiebe*, 2001; *Piontek et al.*, 2009]. Growth of isolated marine bacterial strains, for example, follows Arrhenius' law over a wide range of temperatures (–5 to 30°C) [*Pomeroy and Wiebe*, 2001, and references therein]. Consequently, rising temperatures would have a significant impact on the growth and metabolism of the bacterial community, as well as on protein degrading enzymes, which in turn could lead to a substantial increase in the remineralization rate of POM. Due to significant N isotopic fractionation during OM decomposition (ranging from −3‰ to 1‰), and other related

processes [e.g., *Owens*, 1985; *Ostrom et al*., 1997; *Kendall et al*., 2007], increasing temperatures will act as an important control on $\delta^{15}N_{PN}$ variability. This is clearly supported by the relatively enriched $\delta^{15}N_{PN}$ but much lower PN concentrations in warmer (2015) than usual (2014) years. Clearly, further work on the degradation rates of POM and associated N isotope fractionation is required to confirm the importance of these processes.

Our attempt to use the open-system Rayleigh fractionation equation to calculate the N isotope effect during microbial degradation of POM was complicated by the presence of additional POM sources and/or abiotic processes. For example, intense physical sediment–water interactions and the resuspension of sediments could have an effect on the seasonal dynamics of POM in the PRE, particularly in the dry season when the estuary is well mixed [*Harrison et al*., 2008; *Ye et al*., 2016]. This is partly confirmed by the isotopically similar PN and sedimentary TN along the estuary during the dry season (Figure 6). However, due to the low concentrations of SPM, it seems that sediment resuspensions have only limited contribution to the POM dynamics during our study period. Moreover, active NH_4^+ absorption onto particles in suspension occurs at low salinities during wet periods, as reflected by the slightly positive intercept in the plots of %POC versus %PN (the %PN intercept is between −0.09 and +0.15% at %POC = 0, data not shown). During the absorption process, ^{15}N-enriched NH_4^+ is retained selectively at the exchange sites on SPM [*Delwiche and Steyn*, 1970; *Koba et al*., 2012]. This hypothesis is consistent with the depleted $\delta^{15}N_{NH4}$ but enriched $\delta^{15}N_{PN}$ observed in low-salinity waters during the summer [*Ye et al*., 2016]. A conceptual diagram shows the effects of different sources and processes on POM in the PRE (Figure 12).

Another question of interest is why the water temperature in our study region is much higher in 2015 than 2014 for most seasons (spring and autumn). This is likely to be a response to strong El Niño forcing, which was fully established in spring 2015, and reached its peak strength during November–December 2015 [*Varotsos et al*., 2016; *Zhai et al*., 2016]. It is well established that inter-annual sea surface temperature (SST) variability in the PRE and the adjacent SCS is largely influenced by El Niño conditions, through El Niño-related atmospheric and oceanic changes (e.g., circulation) [*Wang et al*., 2002; *Tang et al*., 2006]. Several studies have suggested that the SCS SST reaches a maximum value about 5 months after the mature phase of El Niño [*Wang et al*., 1997; *Rong et al*., 2007]; however, *Wang et al*. [2002] found that abnormally warm SST in the SCS is in phase with El Niño during the 1997–1998 El Niño year, whereas the SST response lagged the El Niño Southern Oscillation (ENSO) by 1–2 months in the PRE [*Tang et al*., 2006]. This is further evidenced by the occurrence of red tides in early spring along the coasts of Guangdong and Hong Kong [*Yin et al*., 1999; *Deng et al*., 2005]. Additionally, the ENSO potentially affects our study region via ENSO-induced anomalies in rainfall and runoff, such as in late spring 2015, when the Pearl River watershed experienced greater than average precipitation.

Overall, our data suggest that surface water temperature is a primary control on the seasonal dynamics of PN. It can also be inferred that POM dynamics in our study region may accelerate in response to a changing (warming) climate in the future. Recent increases of 0.19–0.34°C per decade in sea surface temperatures over the PRE and adjacent coastal waters already impacting the physical and ecological systems in this region [*Tang et al*., 2006; *Ning et al*., 2009], and temperatures are likely to continue to increase over the next several decades. Previous studies also indicate that riverine fluxes of nutrient and sediment (from the Pearl River) will increase in future [*Li et al*., 2011]. These changes, accompanied by the continued human-induced pressures (i.e., eutrophication), will lead to enhanced cycling of POM in this large subtropical estuary.

4.3. Potential Impacts of Episodic, High Intensity Flood Events

Episodic, high intensity events (e.g., storms and flooding) have typical durations of one to several days; however, the physical and biological responses to these perturbations can last for more than 1–2 weeks [*Fogel et al*., 1999; *Eyre and Ferguson*, 2006]. Although the flood of 2015 was comparatively small relative to the most extreme event in the long-term record (the highest flow ever recorded was 68,500 $m^3\ s^{-1}$ for Xijiang and Beijiang combined), a flood of this kind, with an intermediate frequency, has the highest potential for exporting material to the ocean [*Wheatcroft et al*., 2010; *Tesi et al*., 2013]. Moreover, flooding events influence multiple interrelated processes that could ultimately affect POM dynamics, such as shortening water residence times and increasing the stability of the water column, among other effects. In addition, extremely high discharge during this period pushed the nutrient-rich Pearl River plume farther seaward and formed a salt-wedge estuary. The relatively stable water column and improved light penetration allowed

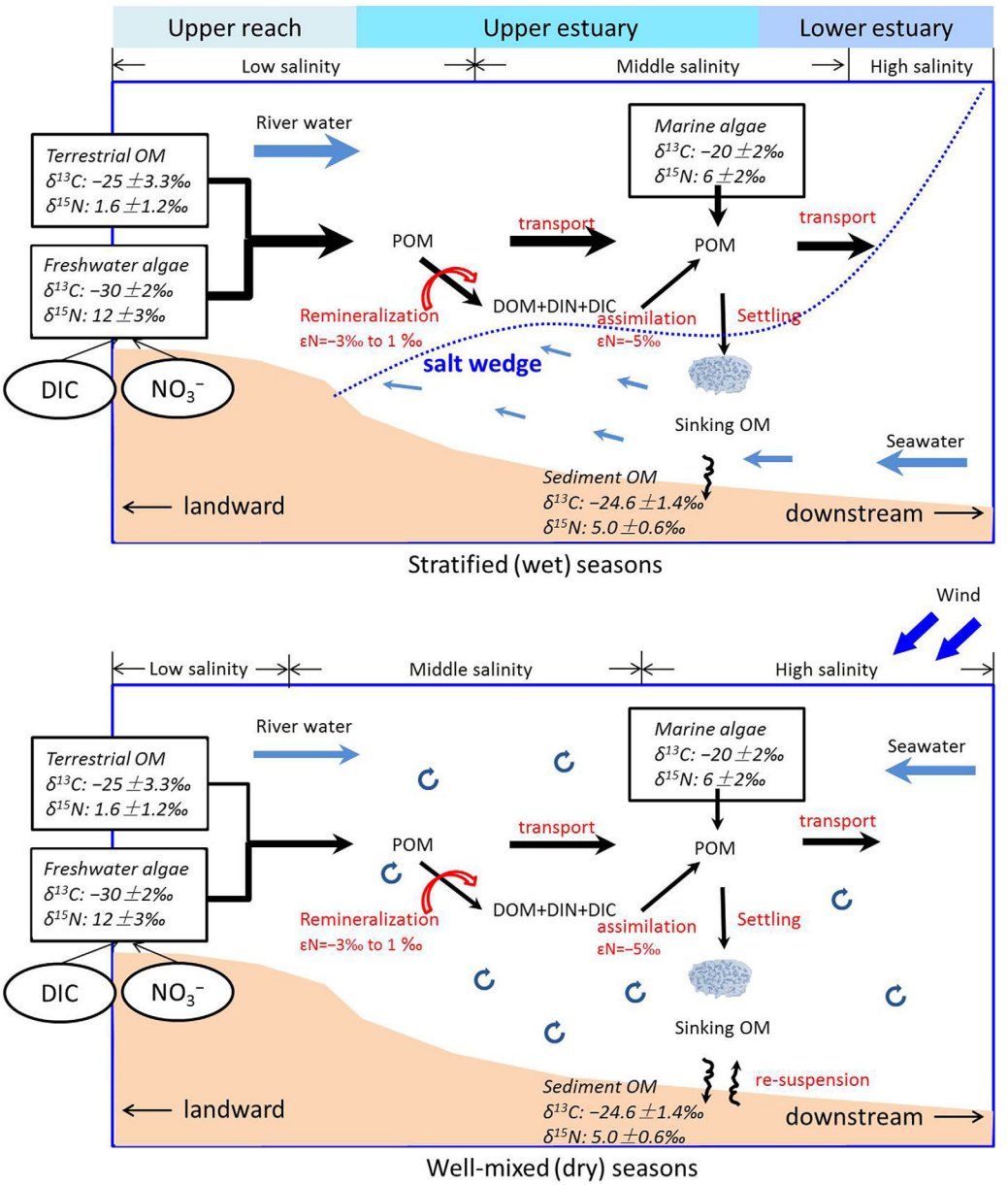

Figure 12. Schematic of the sources and biogeochemical processes of POM in the PRE at different seasons based on $\delta^{13}C$ and $\delta^{15}N$ values.

algal blooms to occur in the coastal region of the estuary, where phytoplankton growth rates were much higher than the water turnover rate [*Dai et al.*, 2008b; *Lu and Gan*, 2015].

A sharp decrease in NO_3^- concentrations was observed after the flooding (Figure 7), presumably due to the dilution of the NO_3^--rich base-flow with NO_3^--poor rainwater [*Fang et al.*, 2011b], which is consistent with the results reported for other watersheds around the world [e.g., *Tesi et al.*, 2013]. The large differences in river discharge were expected to increase nutrient input into the PRE [*Lu et al.*, 2009]. Phytoplankton biomass (*Chl a*) after flooding had nearly doubled compared with preflooding values at middle salinities ($10 < S < 25$). In contrast, freshwater flooding has almost no apparent effect on the concentration of SPM compared with spring (early wet seasons), which has relatively high levels of SPM. It is, however, noteworthy that the observed bloom is different from that of the *Chl a* maximum in the outer estuary (with intermediate salinities) in summer, the latter being related to low SPM concentrations (3.0–6.1 mg L^{-1}, particle size > 0.45 μm) and increased light penetration (1% light depth: 4–6 m) [*Chen et al.*, 2004; *Yin et al.*, 2004]. However, SPM concentrations are several times higher (15.8–22.1 mg L^{-1}, > 0.70 μm) in the lower estuary and

adjacent coastal waters after the flood, as compared with the summer period, which may to some degree limit algal growth due to light limitation. Alternately, the bloom could be due to a greater volume of nutrient-rich water from the enhanced terrestrial runoff and water column stability ($\Delta S > 10$), which are known to be necessary conditions for the formation of a bloom [*Harrison et al*., 2008; *Lu and Gan*, 2015]. The elevated algal biomass had a great impact on $\delta^{15}N_{PN}$ by providing an additions source of $\delta^{15}N$-depleted POM, because phytoplankton preferentially incorporates light isotopes (^{14}N) over heavy isotopes (^{15}N). Additional support for this influence is provided by the isotopically heavy $\delta^{13}C$ data. A similar pattern has been observed in the eutrophic Chesapeake Bay where $\delta^{15}N$ of PN decreased by 3‰–4‰ following a major storm, owing to the enhanced production of phytoplankton in some regions of the bay [*Montoya et al*., 1991]. Overall, our data clearly indicate that the stable isotope signatures of POM changed rapidly, and recorded the physical and biological perturbations within the water column in coastal areas after the short-term flood, which could be important in estimating annual loads of particulate material exported by rivers, and might therefore influence the sedimentary record of OM in estuarine and coastal marine environments.

5. Conclusions

The PRE is a highly dynamic estuarine system flowing into the northern SCS, and it is therefore important to better characterize the sources and biological processing of POM during transport from the land to the sea. Our study reveals that both the quantity and quality of bulk POC and PN, and the contributions from terrestrial OM and in situ marine phytoplankton vary significantly among different seasons and years. Phytoplankton produced in situ is an important source of marine POM in low discharge seasons, whereas terrestrial OM inputs dominate during periods of intense rainfall and high discharge, as indicated by $\delta^{13}C$. The seasonal variability in POM dynamics within the estuary is mainly controlled by seasonally variable water discharge and temperature-modulated biological processes, which are most likely related to NO_3^- assimilation by phytoplankton and microbial degradation. Our data also suggest that seasonal flooding has a profound effect on POM dynamics in the PRE, due to a combination of high discharge and enhanced water column stability. In conclusion, this study clarifies the importance of seasonally variable water discharge and temperature for POM dynamics in large human-perturbed estuarine systems.

Acknowledgments

We would like to thank the captain and the crew of Yue Dongguan 00589 for their excellent support, and Zhijie Liu, Yang Bai, Ruihuan Li, and Xiangfu Li for their help in sampling. The journal editor S. Bradley Moran and two anonymous reviewers are acknowledged for their helpful suggestions and constructive comments on an earlier version of this manuscript. The English of the manuscript was improved by Stallard Scientific Editing. This research was funded by the National Key R&D Program of China (2016YFA0601204), the National Natural Science Foundation of China (41325012, 41306102, and 41506095), and the GIGCAS 135 Project (Y234091001). This is contribution IS-2408 from GIGCAS. A subset of this data set was previously published by *Guo et al*. [2015] and *Ye et al*. [2016]. The data for this paper are available as the supporting information Table S1.

References

Brooks, P. D., P. A. Haas, and A. K. Huth (2007), Seasonal variability in the concentration and flux of organic matter and inorganic nitrogen in a semiarid catchment, San Pedro River, Arizona, *J. Geophys. Res.*, *112*, G03S04, doi:10.1029/2006JG00275.

Brown, J. H., J. F. Gillooly, A. P. Allen, V. M. Savage, and G. B. West (2004), Toward a metabolic theory of ecology, *Ecology*, *85*, 1771–1789.

Cai, Y., X. Ning, and Z. Liu (2002), Studies on primary production and new production of the Zhujiang Estuary [in Chinese with English abstract], China, *Acta Oceanol. Sin.*, *24*, 101–111.

Cai, Y., L. Guo, X. Wang, S. E. Lohrenz, and A. K. Mojzis (2013), Effects of tropical cyclones on river chemistry: A case study of the lower Pearl River during Hurricanes Gustav and Ike, *Estuarine Coastal Shelf Sci.*, *129*, 180–188.

Callahan, J., M. Dai, R. F. Chen, X. Li, Z. Lu, and W. Huang (2004), Distribution of dissolved organic matter in the Pearl River Estuary, China, *Mar. Chem.*, *89*, 211–224.

Canuel, E. A., and A. K. Hardison (2016), Sources, ages and alternation of organic matter in estuaries, *Annu. Rev. Mar. Sci.*, *8*, 409–434.

Cao, Y., G. Sun, G. Xing, and H. Xu (1991), Natural abundance of 15N in main N containing chemical fertilizers of China, *Pedosphere*, *1*, 377–382.

Chen, F., and G. Jia (2009), Spatial and seasonal variations in $\delta^{13}C$ and $\delta^{15}N$ of particulate organic matter in a dam-controlled subtropical river, *River Res. Appl.*, *25*, 1169–1176.

Chen, F., G. Jia and J. Chen (2009), Nitrate sources and watershed denitrification inferred from nitrate dual isotopes in the Beijiang River, south China, *Biogeochemistry*, *94*, 163–174.

Chen, F., L. Zhang, Y. Yang, and D. Zhang (2008), Chemical and isotopic alternation of organic matter during early diagenesis: Evidence from the coastal area off-shore the Pearl River estuary, south China, *J. Mar. Syst.*, *74*, 372–380.

Chen, J., F. Li, and H. Hong (1988), A study on suspended particulate matter in the Zhujiang River estuarine area II. origin, distribution and transport of particulate organic carbon and nitrogen [in Chinese with English abstract], *Trop. Oceanol.*, *7*(3), 90–98.

Chen, J., Y. Li, K. Yin, and H. Jin (2004), Amino acids in the Pearl River Estuary and adjacent waters: Origins, transformation and degradation, *Cont. Shelf Res.*, *24*, 1877–1894.

Cifuentes, L. A., J. H. Sharp, and M. L. Fogel (1988), Stable carbon and nitrogen isotope biogeochemistry in the Delaware estuary, *Limnol. Oceanogr.*, *33*, 1102–1115.

Dai, M., L. Wang, X. Guo, W. Zhai, Q. Li, B. He, and S. J. Kao (2008a), Nitrification and inorganic nitrogen distribution in a large perturbed river/estuarine system: The Pearl River Estuary, China, *Biogeosciences*, *5*, 1227–1244.

Dai, M., et al. (2008b), Effects of an estuarine plume-associated bloom on the carbonate system in the lower reaches of the Pearl River estuary and the coastal zone of the northern South China Sea, *Cont. Shelf Res.*, *28*, 1416–1423.

Delwiche, C. C., and P. L. Steyn (1970), Nitrogen isotope fractionation in soils and microbial reactions, *Environ. Sci. Technol.*, *4*, 929–935.

Deng, S., C. Tang, and D. You (2005), Analysis of abnormally high SST in the red tide sea areas of Guangdong and Hong Kong in the winter-spring of 1998 [in Chinese with English abstract], *Mar. Sci. Bull.*, *24(4)*, 17–21.

Dixon, J. L., C. L. Osburn, H. W. Paerl, and B. L. Peierls (2014), Seasonal changes in estuarine dissolved organic matter due to variable flushing time and wind-driven mixing events, *Estuarine Coastal Shelf Sci.*, *151*, 210–220.
Eyre, B. D., and A. J. P. Ferguson (2006), Impact of a flood event on benthic and pelagic coupling in a sub-tropical east Australian estuary (Brunswick), *Estuarine Coastal Shelf Sci.*, *66*, 111–122.
Fang, Y. T., M. Yoh, K. Koba, W. Zhu, Y. Takebayashi, Y. Xiao, C. Lei, J. Mo, W. Zhang, and X. Lu (2011a), Nitrogen deposition and forest nitrogen cycling along an urban-rural transecr in southern China, *Global Change Biol.*, *17*, 872–885.
Fang, Y. T., K. Koba, X. M. Wang, D. Z. Wen, J. Li, Y. Takebayashi, X. Y. Liu, and M. Yoh (2011b), Anthropogenic imprints on nitrogen and oxygen isotopic composition of precipitation nitrate in a nitrogen-polluted city in southern China, *Atmos. Chem. Phys.*, *11*, 1313–1325.
Fogel, M. L., C. Aguilar, R. Cuhel, D. J. Hollander, J. D. Willey, and H. W. Paerl (1999), Biological and isotopic changes in coastal waters by Hurricane Gordon, *Limnol. Oceanogr. 44*(6), 1359–1369.
Gao, L., D. Li, and J. Ishizaka (2014), Stable isotope ratios of carbon and nitrogen in suspended organic matter: seasonal and spatial dynamics along the Changjiang (Yangtze River) transport pathway, *J. Geophys. Res. Biogeosci.*, *119*, 1717–1737.
Grasshoff, K., K. Kremling, and M. Ehrhardt (1999), *Methods of Seawater Analysis*, Wiley-VCH, Weinheim, Germany.
Guo, W., F. Ye, S. Xu, and G. Jia (2015), Seasonal variation in sources and processing of particulate organic carbon in the Pearl River estuary, South China, *Estuarine Coastal Shelf Sci.*, *167*, 540–548.
Harrison, P. J., K. Yin, J. H. W. Lee, J. Gan, and H. Liu (2008), Physical-biological coupling in the Pearl River Estuary, *Cont. Shelf Res.*, *28*, 1405–1415.
He, B., M. Dai, W. Zhai, .L. Wang.K.Wang, J. Chen. J. Lin. A. Han, and Y.Xu (2010), Distribution, degradation and dynamics of dissolved organic carbon and its major compound classes in the Pearl River estuary, China, *Mar. Chem.*, *119*, 52–64.
Hedges, J. I., R. G. Keil, and R. Benner (1997), What happens to terrestrial organic matter in the ocean, *Organ. Geochem.*, *27*, 195–212.
Hoffman, J. C., and D. A. Bronk (2006), Interannual variation in stable carbon and nitrogen isotope biogeochemistry of the Mattaponi River, Virginia, *Limnol. Oceanogr. Methods*, *51*, 2319–2332.
Hu, J., P. Peng, G. Jia, B. Mai, and G. Zhang (2006), Distribution and sources of organic carbon, nitrogen and their isotopes in sediments of the subtropical Pearl River estuary and adjacent shelf, Southern China, *Mar. Chem.*, *98*, 274–285.
Jia, G.D., and P.A. Peng (2003), Temporal and spatial variations in signatures of sedimented organic matter in Lingding Bay (Pearl estuary), South China, *Mar. Chem.*, *82*, 47–54.
Karsh, K. L. (2014), Physiological and environmental controls on the nitrogen and oxygen isotope fractionation of nitrate during its assimilation by marine phytoplankton, PhD thesis, Univ. of Tas., Hobart, Australia.
Kendall, C., S. R. Silva, and V. J. Kelly (2001), Carbon and nitrogen isotopic compositions of particulate organic matter in four large river systems across the United States, *Hydrol. Processes*, *15*, 1301–1346.
Kendall, C., E. M. Elliott, and S. D. Wankel (2007), Tracing anthropogenic inputs of nitrogen to ecosystems, in *Stable Isotopes in Ecology and Environmental Science*, edited by R. H. Michener and K. Lajtha, pp. 375–449, Blackwell Sci., Oxford, U. K.
Kromkamp, J., and J. Peene (1995), Possibility of net phytoplankton primary production in the turbid Schelde Estuary (SW Netherlands), *Mar. Ecol. Prog. Ser.*, *121*, 249–259.
Lara, R. J., V. Alder, C. A. Franzosi, G. Kattner (2010), Characteristics of suspended particulate organic matter in the southwestern Atlantic: influence of temperature, nutrient and phytoplankton features on the stable isotope signature, *J. Mar. Syst.*, *79*, 199–209.
Li, X., Y. Yang, Y. Qiao, X. Zhou, S. Wang, and X. Mai (2015), Temporal-spatial distribution and sources of nitrogen in main stream of Dongjiang River [in Chinese with English abstract], *Acta Sci. Circum.*, *35*, 2143–2149.
Li, Y., B.-M. Chen, Z.-G. Wang, and S.-L. Peng (2011), Effect of temperature change on water discharge, and sediment and nutrient loading in the lower Pearl River basin on SWAT modeling, *Hydrol. Sci. J.*, *56*(1), 68–83.
Liu, C., X. Ning, Y. Cai, Q. Hao, and F. Le (2007), Bacterioplankton production in the Zhujiang River Estuary and the adjacent northern South China Sea [in Chinese with English abstract], *Acta Oceanol. Sin.*, *29*, 112–122.
Liu, K.-K., S.-J. Kao, L.-S. Wen, and K.-L. Chen (2007), Carbon and nitrogen isotopic compositions of particulate organic matter and biogeochemical processes in the eutrophic Danshuei Estuary in northern Taiwan, *Sci. Total Environ.*, *382*, 103–120.
Liu, K.-K., S.-J. Kao, K.-P. Chiang, G.-C. Gong, J. Chang, J.-S. Cheng, and C.-Y. Lan (2013), Concentration dependent nitrogen isotope fractionation during ammonium uptake by phytoplankton under an algal bloom condition in the Danshuei Estuary in northern Taiwan, *Mar. Chem.*, *157*, 242–252.
Loder, T. C., and R. P. Reichard (1981), The dynamics of conservative mixing in estuaries, *Estuaries*, *4*, 64–69.
Lorenzen, C. J. (1967), Determination of chlorophyll and pheopigments: Spectrophotometric equations, *Limnol. Oceanogr.*, *12*, 343–346.
Lu, F. H., H. G. Ni, F. Liu, and E. Y. Zeng (2009), Occurrence of nutrients in riverine runoff of the Pearl River Delta, South China, *J. Hydrol.*, *376*, 107–115.
Lu, Z., and J. Gan (2015), Controls of seasonal variability of phytoplankton blooms in the Pearl River Estuary, *Deep Sea Res., Part II*, *117*, 86–96.
Luo, Y., S. Liu, S. Fu, J. Liu, G. Wang, and G. Zhou (2008), Trends of precipitation in Beijiang River Basin, Guangdong Province, China, *Hydrol. Process.*, *22*, 2377–2386.
Maksymowska, D., P. Richard, H. Piekarek-Jankowska, and P. Riera (2000), Chemical and isotopic composition of the organic matter sources in the Gulf of Gdansk (Southern Baltic Sea), *Estuarine Coastal Shelf Sci.*, *51*, 585–598.
Maya, M. V., S. G. Karapurkar, H. Naik, R. Roy, D. M. Shenoy, and S. W. A. Naqvi (2011), Intra-annual variability of carbon and nitrogen stable isotopes in suspended organic matter in waters of the western continental shelf of India, *Biogeosciences*, *8*, 3441–3456.
McCallister, S. L., J. E. Bauer, J. E. Cherrier, and H. W. Ducklow (2004), Assessing sources and ages of organic matter supporting river and estuarine bacterial production: A multiple-isotope ($\Delta^{14}C$, $\delta^{13}C$, and $\delta^{15}N$) approach, *Limnol. Oceanogr. Methods*, *49*, 1687–1702.
Meybeck, M. (1982), Carbon, nitrogen, and phosphorus transport by world rivers, *Am. J. Sci.*, *282*, 401–450.
Middelburg, J. J., and J. Nieuwenhuize (1998), Carbon and nitrogen stable isotopes in suspended matter and sediments from the Schelde Estuary, *Mar. Chem.*, *60*, 217–225.
Middelburg, J. J., and J. Nieuwenhuize (2000), Nitrogen uptake by heterotrophic bacteria and phytoplankton in the nitrate-rich Thames estuary, *Estuarine Coastal Shelf Sci.*, *203*, 13–21.
Montoya, J. P., S. G. Korrigan, and J. J. McCarthy (1991), Rapid, storm-induced changes in the natural abundance of ^{15}N in a planktonic ecosystem, Chesapeake Bay, USA, *Geochim. Cosmochim. Acta*, *55*, 3627–3638.
Ning, X., C. Lin, Q. Hao, C. Liu, F. Le, and J. Shi (2009), Long term changes in the ecosystem in the northern South China Sea during 1976–2004, *Biogeosciences*, *6*, 2227–2243.
Osburn, C. L., L. T. Handsel, M. P. Mikan, H. W. Paerl, and M. T. Montgomery (2012), Fluorescence tracking of dissolved and particulate organic matter quality in a river-dominated estuary, *Environ. Sci. Technol.*, *46*, 8628–8636.

Ostrom, N. E., S. A. Macko, D. Deibel, and R. J. Thompson (1997), Seasonal variation in the stable carbon and nitrogen isotope biogeochemistry of a coastal cold ocean environment, *Geochim. Cosmochim. Acta*, *61*, 2929–2942.
Owens, N. J. P. (1985), Variations in the natural abundance of 15N in estuarine suspended particulate matter: A specific indicator of biological processing, *Estuarine Coastal Shelf Sci.*, *20*, 505–510.
Phillips, D. L., and J. W. Gregg (2001), Uncertainty in source partitioning using stable isotopes, *Oecologia*, *127*, 171–179.
Phillips, D. L., and J. W. Gregg (2003), Source partitioning using stable isotopes: Coping with too many sources, *Oecologia*, *136*, 261–269.
Phillips, D. L., and J. W. Gregg (2005), Combining sources in stable isotope mixing models: Alternative methods, *Oecologia*, *144*, 520–527.
Piontek, J., N. Handel, G. Langer, J. Wohlers, U. Riebesell, and A. Engel (2009), Effects of rising temperature on the formation and microbial degradation of marine diatom aggregates, *Aquat. Microb. Ecol.*, *54*, 305–318.
Pomeroy, L., and W. J. Wiebe (2001), Temperature and substrates as interactive limiting factors for marine heterotrophic bacteria, *Aquat. Microb. Ecol.*, *23*, 187–204.
Qiu, D., L. Huang, J. Zhang, and S. Lin (2010), Phytoplankton dynamics in and near the highly eutrophic Pearl River Estuary, South China Sea, *Cont. Shelf Res.*, *30*, 177–186.
Rau, G. H., T. Takahashi, D. J. Des Marais, and C. W. Sullivan (1991), Particulate organic matter δ^{13}C variations across the Drake Passage, *J. Geophys. Res.*, *96*, 15131–15135.
Rong, Z., Y. Liu, H. Zong, and Y. Cheng (2007), Interannual sea level variability in the South China Sea and its response to ENSO, *Global Planet. Change*, *55(4)*, 257–272.
Rudek, J., H. W. Paerl, M. A. Mallin, and P. W. Bates (1991), Seasonal and hydrological control of phytoplankton nutrient limitation in the lower Neuse River Estuary, North Carolina, *Mar. Ecol. Prog. Ser.*, *75*, 133–142.
Sato, T., T. Miyajima, H. Ogawa, Y. Umezawa, and I. Koike (2006), Temporal variability of stable carbon and nitrogen isotopic composition of size-fractionated particulate organic matter in the hypertrophic Sumida River Estuary of Tokyo Bay, Japan, *Estuarine Coastal Shelf Sci.*, *68*, 245–258.
Seitzinger, S. P., C. Kroeze, A. F. Bouwman, N. Caraco, F. Dentener, and R. V. Styles (2002), Global patterns of dissolved inorganic and particulate nitrogen inputs to coastal systems: Recent conditions and future projections, *Estuaries*, *25*, 640–655.
Sigman, D. M., M. A. Altabet, D. C. McCorkle, R. Francois, and G. Fischer (1999), The δ^{15}N of nitrate in the Southern Ocean: consumption of nitrate in surface waters, *Global Biogeochem. Cy.*, *13*, 1149–1166.
Sun, H., J. Han, S. Zhang, and X. Lu (2007), The impacts of '05.6' extreme flood event on riverine carbon fluxes in Xijiang River, *Chin. Sci. Bull.*, *52*, 805–512.
Sun, J., B. Lin, K. Li, and G. Jiang (2014), A modelling study of residence time and exposure time in the Pearl River Estuary, China, *J. Hydro-Environ. Res.*, *8*, 281–291.
Sweeney, R. E., E. K. Kalil, and I. R. Kaplan (1980), Characterization of domestic and industrial sewage in South California coastal sediments using nitrogen, carbon, sulphur and uranium tracers, *Mar. Environ. Res.*, *3*, 225–243.
Tang, C., Z. Zheng, D. Wei, S. Deng, and Y. Huang (2006), Analysis of SST variation in recent 30 years in the Zhujiang River estuary [in Chinese with English abstract], *J. Oceanogr. Taiwan Str.*, *25*, 96–101.
Tesi, T., S. Miserocchi, F. Acri, L. Langone, A. Boldrin, J. A. Hatten, and S. Albertazzi (2013), Flood-driven transport of sediment, particulate organic matter, and nutrients from the Po River watershed to the Mediterranean Sea, *J. Hydrol.*, *498*, 144–152.
Thornton, S. F., and J. McManus (1994), Application of organic carbon and nitrogen stable isotope and C/N ratios as source indicators of organic matter provenance in estuarine systems: Evidence from the Tay Estuary, Scotland, *Estuarine Coastal Shelf Sci.*, *38*, 219–233.
Varotsos, C. A., C. G. Tzanis, and N. V. Sarlis (2016), On the progress of the 2015–2016 El Niño event, *Atmos. Chem. Phys.*, *16*, 2007–2011.
Wang, D., Z. Qin, and F. Zhou (1997), Study on air-sea interaction on the interannual time-scale in the South China Sea [in Chinese with English abstract], *Acta Meteorol. Sin.*, *55*(1), 33–42.
Wang, D., Q. Xie, Y. Du, W. Wang, and J. Chen (2002), The 1997–1998 warm event in the South China Sea, *Chin. Sci. Bull.*, *47*(14), 1221–1227.
Wang, D., W. Lin, X. Yang, W. Zhai, M. Dai, and C.-T. A. Chen (2012), Occurrence of dissolved trace metals (Cu, Cd, and Mn) in the Pearl River Estuary (China), a large river-groundwater-estuary system, *Cont. Shelf Res.*, *50/51*, 54–63.
Wang, S. (2014), Submarine groundwater discharge and associated fluxes of nutrients and carbon into the Pearl River estuary, Master thesis, Univ. of Xiamen, Xiamen, China.
Wang, X.-C., R. F. Chen, and G. B. Gardner (2004), Sources and transport of dissolved and particulate organic carbon in the Mississippi River estuary and adjacent coastal waters of the northern Gulf of Mexico, *Mar. Chem.*, *89*, 241–256.
Wei, X., C. Shen, Y. Sun, and W. Yi (2008), The study of stable carbon isotope composition of riverine suspended matter and soil erosion of the Pearl River Drainage Basin [in Chinese with English abstract], *Acta Sediment. Sin.*, *26*, 151–157.
Wheatcroft, R. A., M. A. Goni, J. A. Hatten, G. B. Pasternack, and J. A. Warrick (2010), The role of effective discharge in the ocean delivery of particulate organic carbon by small, mountainous river systems, *Limnol. Oceanogr. Methods*, *55*, 161–171.
Wu, Y., J. Zhang, S. M. Liu, Z. F. Zhang, Q. Z. Yao, G. H. Hong, and L. Cooper (2007), Sources and distribution of carbon within the Yangtze River system, *Estuarine Coastal Shelf Sci.*, *71*, 13–25.
Ye, F., G. Jia, L. Xie, G. Wei, and J. Xu (2016), Isotope constraints on seasonal dynamics of dissolved and particulate N in the Pearl River Estuary, south China, *J. Geophys. Res. Oceans 121*, 8689–8705, doi:10.1002/2016JC012066.
Yin, K., P. J. Harrison, J. C. Chen, W. Huang, and P. Y. Qian (1999), Red tides during spring 1998 in Hong Kong: Is El Niño responsible?, *Mar. Ecol. Prog. Ser.*, *187*, 289–294.
Yin, K., P. Y. Qian, J. C. Chen, D. P. H. Hsieh, and P. J. Harrison (2000), Dynamics of nutrients and phytoplankton biomass in the Pearl River estuary and adjacent waters of Hong Kong during summer: Preliminary evidence for phosphorus and silicon limitation, *Mar. Ecol. Prog. Ser.*, *194*, 295–305.
Yin, K., J. Zhang, P.-Y. Qian, W. Jian, L. Huang, J. Chen, and M. C. S. Wu (2004), Effect of wind events on phytoplankton blooms in the Pearl River estuary during summer, *Cont. Shelf Res.*, *24*, 1909–1923.
Yu, F., Y. Zong, J. M. Lloyd, G. Huang, M. J. Leng, C. Kendrick, A. L. Lamb, W. W.-S. Yim (2010), Bulk organic and C/N as indicators for sediment sources in the Pearl River delta and estuary, southern China, *Estuarine Coastal Shelf Sci.*, *87*, 618–630.
Zhai, P., R. Yu, Y. Guo, Q. Li, X. Ren, Y. Wang, W. Xu, Y. Liu, and Y. Ding (2016), The strong El Niño of 2015/16 and its dominant impacts on global and China's climate, *J. Meteorol. Res.*, *30*, 283–297.
Zhang, J., Z. G. Yu, J. T. Wang, J. L. Ren, H. T. Chen, H. Xiong, L. X. Dong, and W. Y. Xu (1999), The subtropical Zhujiang (Pearl River) Estuary: Nutrient, trace species and their relationship to photosynthesis, *Estuarine Coastal Shelf Sci.*, *49*, 385–400.
Zhang, Q., V. P. Singh, J. Peng, Y. D. Chen, and J. Li (2012), Spatial-temporal changes of precipitation structure across the Pearl River basin, China, *J. Hydrol.*, *440/441*, 113–122.

Zhang, Y., Q. Gao, X. Huang, Z. Wang, G. Yao, T. He, J. Ding and H. Zhong (2007), The response of dissolved organic carbon export to the typical flood event in the Xijiang River [in Chinese with English abstract], *Acta Sci. Circum.*, *27*, 143–150.

Zhang, Y., K. Kaiser, L. Li, D. Zhang, Y. Ran, and R. Benner (2014), Sources, distributions, and early diagenesis of sedimentary organic matter in the Pearl River region of the South China Sea, *Mar. Chem.*, *158*, 39–48.

Zhao, X., F. Chen, J. Chen, C. Tang, Y. Luo, and G. Jia (2008), Using nitrogen isotope to identify the sources of nitrate contamination in urban groundwater-a case study in Zhuhai city [in Chinese with English abstract], *Hydrogeol. Eng. Geol.*, *3*, 87–92.